2017

Characterization of a H4K20ME2 Methyl-Binding Domain in the Fanconi Anemia Protein FANCD2

Karissa Lynn Paquin
University of Rhode Island, karissa_neira@uri.edu

CHARACTERIZATION OF A H4K20ME2 METHYL-BINDING DOMAIN IN THE FANCONI ANEMIA PROTEIN FANCD2

BY

KARISSA LYNN PAQUIN

A DISSERTATION SUBMITTED IN PARTIAL FULFILLMENT OF THE

REQUIREMENTS FOR THE DEGREE OF

DOCTOR OF PHILOSOPHY

IN

CELL AND MOLECULAR BIOLOGY

UNIVERSITY OF RHODE ISLAND

2017

DOCTOR OF PHILOSOPHY DISSERTATION

OF

KARISSA LYNN PAQUIN

APPROVED:

Dissertation Committee:

Major Professor Niall Howlett

Jodi Camberg

Abraham Kovoor

Nasser H. Zawia
DEAN OF THE GRADUATE SCHOOL

UNIVERSITY OF RHODE ISLAND
2017

ABSTRACT

Fanconi anemia (FA) is a rare genetic disease that results on early onset bone marrow failure, congenital defects, and increased cancer susceptibility. It is caused by mutation in any one of twenty two genes, whose protein products work in conjunction as part of the FA-BRCA pathway, a DNA repair pathway that specifically repairs DNA interstrand crosslinks (ICLs). One of the key steps in pathway activation is the monoubiquitination of the FANCD2 protein. Upon pathway activation, FANCD2 is recruited to sites of DNA damage, where is interacts with downstream repair protiens to promote DNA repair *via* homologous recombination (HR). How FANCD2 recognizes DNA damage in condensed compact chromatin, however, has remained unknown. Here, we uncover a FANCD2 methyl-binding domain, which specifically binds for H4K20me2 in order to recruit FANCD2 to sites on DNA damage and promote homologous recombination, support cell survival and maintain genomic integrity.

ACKNOWLEDGMENTS

I would first like to thank my PI and dissertation advisor, Dr. Niall G. Howlett for affording me the opportunity to work in his lab. The guidance and advice I have received throughout the years has been invaluable not only to the completion of my dissertation, but also to my future career in research. While the knowledge I have gained through my research has been extensive, my personal growth and critical thinking skills overshadow that greatly, in large part to your guidance and perseverance, even on days where I was ready to throw in the towel. I would also like to thank my committee member Dr. Abraham Kovoor for feedback on my dissertation and advice throughout my graduate career. Thank you to Dr. Allison Roberts for giving time and feedback towards chairing my comprehensive exam and dissertation defense. I would like to extend many thanks to Dr. Jodi Camberg, not only for giving advice and feedback during committee meetings and on proposal, comprehensive exam, and dissertation drafts, but for participating in many impromptu meetings on my dissertation research, and extending a helping hand in optimization and design of assays as well as guiding my research.

I would like to thank Paul Azzinarro and Nicholas Mamrak for their hard work and dedication to multiple aspects of my project, and for their contributions to Manuscript II.

I would also like to thank the many members of the Howlett lab that I have worked with throughout the years. Your support through presentation run-throughs, paper proof-reading, poster design, lab meetings, and experimental feedback has been vital to my research and success in graduate school. I would especially like to thank Dr. Elizabeth Vuono and soon-to-be Dr. David Vierra for not only the aforementioned help,

but also being amazing and supportive friends throughout my graduate career. Your celebrations of exciting data, and supportive pep talks during times of frustration have been essential to my sanity throughout this entire process.

To the department of Cell and Molecular Biology at URI, thank you for your guidance and support throughout the years.

Lastly, I would like to thank my family. To my parents, thank you for raising me to believe I could do anything I could set my mind to, and teaching me the importance of education. Additionally, I could not have made it through the graduate program without the mental and physical support you've provided throughout the years. A huge thank you to my husband Ryan, for (almost) never complaining of the long hours I spent in the lab or late at night working, and providing a huge mental support while I worked through my dissertation work. I could not have done this without your full support, your confidence in me, and your hard work to keep our family afloat. Finally, I would like to acknowledge my sweet daughter, Braelynn, and her future younger sibling, who have kept me motivated to set the best example I can through pursuing my dreams, while trying to somehow change this world for the better. Your intelligence astounds me, and your sweet smile and laugh have given comfort when the going has gotten tough. I love you all.

PREFACE

The following dissertation has been prepared in manuscript format. Chapter 1, "The role of histone H4 lysine 20 Dimethylation (H4K20me2) in the repair of DNA double strand breaks" was prepared for publication in *Nucleic Acids Research* and is a review on the regulation, role, and recognition of dimethylated H4K20 in DNA double strand break repair. Chapter 2, "FANCD2 binding to H4K20me2 *via* a methyl-binding domain is essential for efficient DNA crosslink repair" was prepared for publication in *Proceedings of the National Aacademy of Sciences*.

TABLE OF CONTENTS

LIST OF FIGURES

MANUSCRIPT I

MANUSCRIPT II

APPENDIX II

FIGURE PAGE

Manuscript-I

Prepared for submission to Nucleic Acids Research

The histone DNA repair code: H4K20me2 makes its mark

Karissa L Paquin and Niall G Howlett

Department of Cell and Molecular Biology, University of Rhode Island, Kingston, Rhode Island, U.S.A

Corresponding Author: Niall G. Howlett, Ph.D.

Department of Cell and molecular biology

University of Rhode Island

379, CBLS, 120 Flagg Rd.

Kingston, RI, 02881, USA

Phone: +1-401-874-4306

Email address: nhowlett@uri.edu

The histone DNA repair code: H4K20me2 makes its mark

Karissa L. Paquin[a] and Niall G. Howlett[a,1]

[a]Department of Cell and Molecular Biology, University of Rhode Island, Kingston, Rhode Island, U.S.A

[1]Corresponding author: Niall G. Howlett Ph.D., 379 Center for Biotechnology and Life Sciences, 120 Flagg Road, Kingston, RI, USA, Tel.: +1 401 874 4306; Fax: +1 401 874 2065; *Email address*: **nhowlett@uri.edu**

Keywords: H4K20me2, DNA DSB repair, histone posttranslational modification, homologous recombination, nonhomologous DNA end joining

Abstract

Chromatin is a highly compact structure that must be rapidly rearranged in order for DNA repair proteins to access sites of damage and facilitate timely and efficient repair. Chromatin plasticity is achieved through multiple processes, including the posttranslational modification of histone tails. In recent years, the impact of histone posttranslational modification on the DNA damage response has become increasingly well recognized, and chromatin plasticity has been firmly linked to efficient DNA repair. One particularly important histone posttranslational modification is the methylation of H4K20. Here we discuss the regulation and function of H4K20 methylation (H4K20me) in the DNA damage response: we describe the *writers*, *erasers*, and *readers* of this important chromatin mark, and discuss combinatorial histone posttranslational modifications that modulate H4K20me recognition. Finally, we discuss the central role of H4K20me in determining whether DNA double-strand breaks are repaired by the error-prone nonhomologous DNA end joining or error-free homologous recombination pathways.

Introduction

Chromatin is a highly organized and condensed structure that allows billions of base pairs of DNA to be tightly packaged into the nuclei of eukaryotic cells. The basic subunit of chromatin is the nucleosome, an octamer of histones around which 146 bp of DNA is wrapped almost twice. Each nucleosome contains two copies each of histones H2A, H2B, H3, and H4. Histones are highly conserved amongst eukaryotes, emphasizing their importance (1). Chromatin cannot be a rigid and unchanging structure, however. It is

highly dynamic in order to facilitate DNA replication, transcription, and repair. Chromatin plasticity is a necessity, as without it, DNA interacting proteins would not be able to access this tightly condensed structure. Chromatin plasticity is facilitated by nucleosome repositioning, histone exchange, and the post-translational modification (PTM) of histone tails. Nucleosome repositioning involves the physical sliding of nucleosomes along the DNA or their eviction. In histone exchange, histone variants are substituted for the canonical histones H2A, H2B, H3 or H4. For example, H2A can be substituted for the variant H2AX upon the formation of DNA double-strand breaks (DSBs) (2). Histone PTM is the addition of small molecules, such as acetyl-, methyl-, and phospho-groups, or small proteins, such as SUMO (small ubiquitin-like modifier) and ubiquitin to the tails of histones, which extend from the core nucleosome. These PTMs change chromatin structure in several ways, for example, by modulating the strength of histone-DNA interactions, and by facilitating the recruitment of chromatin *reader* proteins and/or chromatin remodeling complexes, which can lead to marked changes in chromatin structure and compaction. Single and combinatorial PTMs can have distinct signaling and cellular outcomes. Combinatorial marks add to the variability and complexity of chromatin recognition and plasticity (3,4). In this review, we will focus on one aspect of chromatin plasticity, namely histone PTM. Specifically, we will discuss the methylation of histone H4 lysine 20 and how this particular PTM has become increasingly recognized as a major determinant of DNA repair.

DNA Double-Strand Break Repair

DNA damage can arise as a result of endogenous agents, such as reactive oxygen species, a byproduct of normal cellular processes, or by exogenous means, such as exposure to UV light. DNA damage must be repaired in an efficient and timely manner in order to continue normal cellular processes like replication and transcription. While there are many types of DNA damage, here we will focus on DNA double-strand breaks (DSBs). DSBs arise upon cellular exposure to ionizing radiation and as a consequence of replication fork collapse. DSBs can also arise transiently during DNA repair processes, including nucleotide excision repair and interstrand crosslink repair (5). Upon DSB formation, free ends of broken DNA are recognized by the MRN (MRE11-RAD50-NBS1) complex, which recruits the ATM (ataxia telangiectasia mutated) kinase (6,7). ATM phosphorylates a histone variant called H2AX on serine 139, forming γH2AX (8,9). γH2AX was one of the first recognized histone PTMs, and has been extensively studied in relation to DSB repair (8). MDC1 (mediator of DNA damage checkpoint 1) recognizes γH2AX *via* its BRCT (BRCA1 C-Terminus) domain (10). MDC1 subsequently recruits additional molecules of ATM *via* its FHA (forkhead-associated) domain; ATM phosphorylates additional H2AX molecules thereby amplifying the γH2AX signal up to two megabases proximal to the DSB site (10-12) (Figure 1A). As one of the first steps in DSB repair, H2AX phosphorylation is widely used as a marker for DSB formation.

DSBs are repaired by one of two ways: homologous recombination (HR) or non-homologous DNA end joining (NHEJ). Homologous recombination is an error-free repair pathway that uses a homologous DNA sequence as a template to repair damaged

Figure 1. Recognition of the double strand break (DSB), homologous recombination, and nonhomologous DNA end joining. Upon DSB formation, MRE11, RAD50, and NBS1 recognize the free naked ends of DNA, and recruit ATM. ATM phosphorylates H2AX to form γH2AX. MDC1 then recognizes γH2AX, and recruits subsequent molecules of ATM, which in turn phosphorylate additional H2AX. This cascade reaches outward from the broken ends up to 2 megabases of DNA (A). After recognition of DNA damage and phosphorylation of H2AX, BRCA1, CtIP, and EXO1 are all recruited to DSBs, where they promote end resection. Exonuclease activity results in 3' ssDNA overhangs. RAD51 coats the ssDNA, and scans the sister chromatid for a homologous sequence. BRCA1, RAD51, and its associated proteins invade the sister chromatid, forming the displacement loop. New DNA is synthesized off of the sister chromatid, and Holliday junctions are resolved, repairing the broken DNA in an error free manner (B). In the absence of BRCA2, 53BP1 is recruited to DSB sites. It blocks CtIP, and therefore end resection. Ku70/Ku80 are then recruited to these sites, where they signal Artemis and LIG4 localization. The broken ends are then ligated together to repair the break (C).

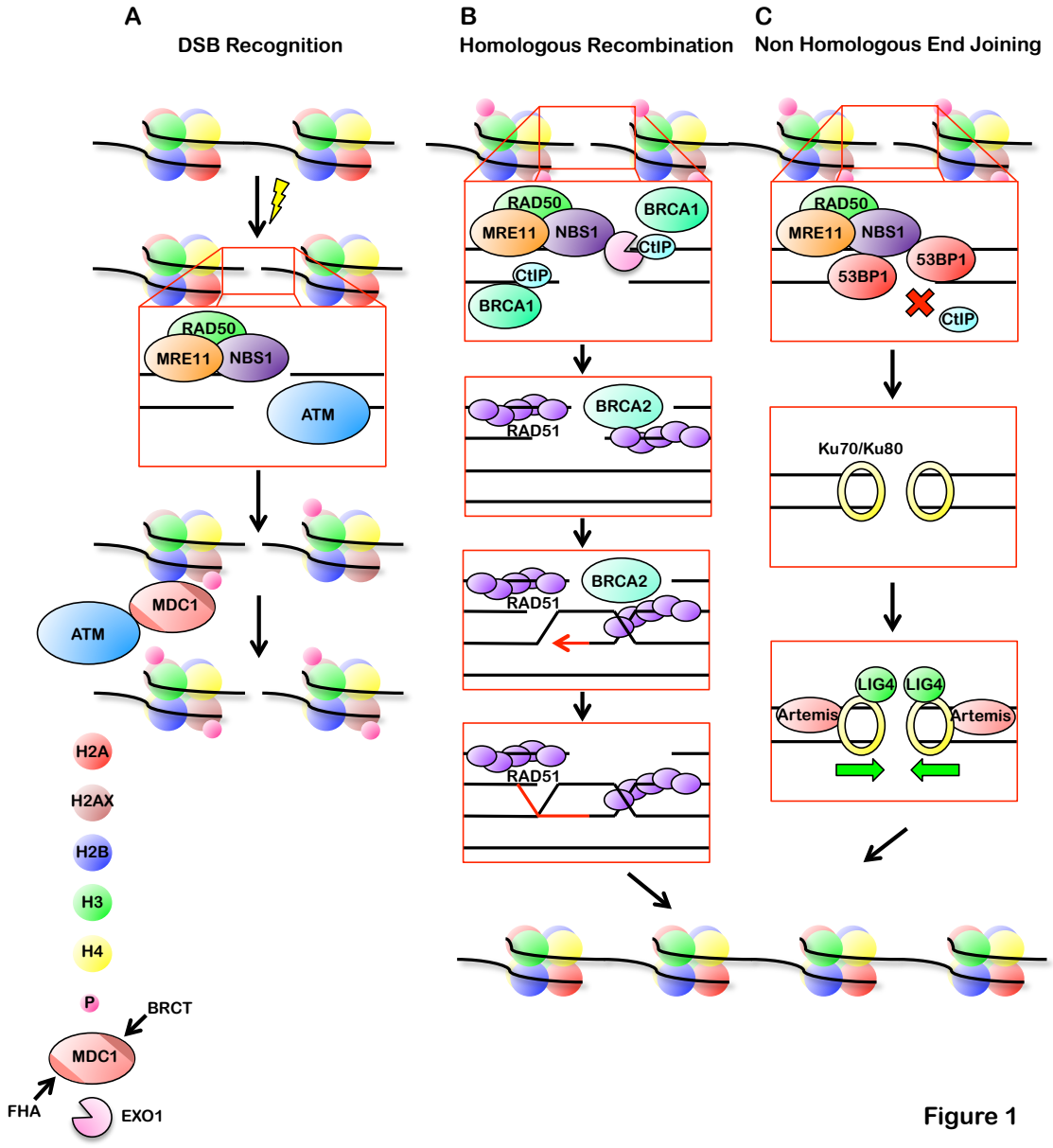
A
DSB Recognition
B
Homologous Recombination
C
Non Homologous End Joining
RAD50
MRE11
NBS1
ATM
MDC1
H2A
H2AX
H2B
H3
H4
P
BRCT
FHA
EXO1
BRCA1
CtIP
RAD51
BRCA2
53BP1
Ku70/Ku80
LIG4
Artemis

Figure 1

DNA (13). It is a cell cycle-dependent pathway, occurring primarily during S-phase due to the presence of homologous DNA in the sister chromatid. Briefly, upon γH2AX phosphorylation, the MRN complex, CtIP (CtBP-interacting protein), EXO1 (exonuclease 1), and DNA2 (DNA replication/helicase protein 2) all promote 5'-3' DNA end resection, resulting in the generation of 3' single-stranded overhangs on each strand (ssDNA) (14-18). These ssDNA overhangs are first coated by RPA (replication protein A) to protect against nucleolytic degradation. The major DNA strand recombinase, RAD51, is subsequently loaded onto ssDNA in a process facilitated by functional homologs of the yeast Rad52 epistasis group and the BRCA2 protein (19-21). RAD51 forms a nucleoprotein filament coating the ssDNA and a displacement loop (D-loop) is formed upon invasion of the ssDNA into the complementary sister chromatid duplex, referred to as the synaptic complex (19-23). New DNA is then synthesized using the sister chromatid as a template, and Holliday junctions (DNA intermediates that contain a crossover between newly synthesized DNA on the invading strand and the template strand) are resolved, resulting in a duplicate of the sister chromatid (gene conversion), with no loss of genetic information (13) (Figure 1B).

On the other hand, NHEJ is typically an error-prone pathway that simply ligates the free ends of broken DNA. NHEJ occurs in all phases of the cell cycle, and can result in catastrophic events such as deletions and translocations. In brief, again MRN is recruited to DSBs after damage. Additionally, 53BP1 (p53 Binding Protein 1) is recruited to DNA damage sites, and blocks HR proteins and end resection (24,25). Ku70 (Lupus Ku auto antigen p70) and Ku80 (Lupus Ku auto antigen p86) recognize the DSB ends and together with DNA-PKcs (DNA-dependent protein kinase catalytic subunit), Artemis,

XRCC4 (X-ray repair cross-complementing protein 4), and LIG4 (DNA ligase 4), directly ligate the free ends of the DSB (26-30) (Figure 1C). Often, there is no specificity for which ends are ligated, which can result in translocations if ends from two distinct DSBs are rejoined (31,32).

There are many factors that determine whether HR or NHEJ is used to repair a DSB. While cell cycle plays an important role in DNA repair pathway decision, there are multiple factors that influence HR vs. NHEJ, and the dynamics of this decision have not been fully elucidated. Two proteins that play a major role in determining if HR or NHEJ is initiated are BRCA1 and 53BP1. While the MRN complex plays a key role in both HR and NHEJ, its binding partners determine whether BRCA1 or 53BP1 becomes loaded onto DSB ends (33). The regulation of this process will be discussed in greater detail later in the review. Depletion of Brca1 results in increased NHEJ and decreased HR (34). Depletion of both Brca1 and 53bp1, however, restores normal levels of HR in mice (25). This, along with evidence that 53BP1 physically blocks end resection, indicates that BRCA1 may play a role in 53BP1 removal from DSB sites, allowing HR to proceed (33).

H4K20me2

KMT5A

Prior to H4K20 di- or tri- methylation, H4K20 must first be monomethylated (35-37). The enzyme responsible for H4K20 monomethylation is KMT5A (lysine methyltransferase 5A), a SET-domain (Su(var)3-9, Enhancer-of-zeste and Trithorax) containing methyltransferase. It has recently been shown that KMT5A prefers the entire nucleosome as its substrate, rather than individual H4 histones or peptides, and that it

interacts with H2A and H2B in order to monomethylate H4K20 (38-41). Loss of Kmt5a in both fly and mouse results in embryonic lethality (42,43). Studies have shown that with knockout of Kmt5a, H4K20 di- and tri- methylation are down regulated (42). In HeLa cells, KMT5A knockdown results in reduced 53BP1 recruitment to DSBs. (44,45). Additionally, Kmt5a knockout embryonic stem cells and KMT5A depleted HeLa and U2OS cells display increased DSBs and γH2AX formation, even in the absence of DNA damaging agents (42,46,47). This is likely an accumulation of spontaneous damage throughout the cell cycle, that remains unrepaired due to lack of H4K20 methylation (42). KMT5A depleted U2OS cells have increased cell cycle checkpoint activation, decreased cell cycle progression, and accumulate in S-phase, also in the absence of DNA damage (47).

KMT5B/C

The H4K20me2 mark has been shown to be involved in DNA repair. This histone mark is found throughout the nucleus, however it has been reported to be enriched at sites of DNA damage (48). Globally, Kmt5b and Kmt5c are responsible for dimethylation and trimethylation, respectively. (49). KMT5B/C has been shown to enzymatically catalyze dimethylation more efficiently than trimethylation *in vitro* (35,36,50). This suggests that additional proteins are necessary for efficient H4K20 trimethylation, or that another HMT catalyzes this reaction (35,49). While *in vitro* studies show that SMYD3, a SET domain containing methyltransferase, is capable of recognizing H4K20me2 and catalyzing the addition of an additional methyl group, depletion of KMT5B/C results in complete lack of H4K20me3 (49,51). KMT5B and KMT5C are unique in that they have leucine and

cysteine substitutions in the two conserved tyrosine residues that regulate substrate specificity in other SET domain containing methyltransferases. However, KMT5B and KMT5C still maintain the characteristic SET-domain structure (35,36). Like many methyltransferases, they require a SAM (S-adenosyl-L-methionine) cofactor to donate a methyl group to the substrate (35,36,49). These enzymes regulate H4K20 dimethylation, and knockdown of Kmt5b/c in fly and Kmt5b/c -/- double knockout MEFs results in decreased H4K20me2/3 (but not H4K20me1) (50). Cells depleted of KMT5B/C and kmt5b/c$^{-/-}$ double knockout MEFs exhibit delayed 53BP1 foci formation, one of several proteins that binds H4K20me2 (50,52,53). The Kmt5b/c methyltransferases have also been linked to DNA repair and genome instability, and play a role in telomere length maintenance and the regulation of heterochromatin compaction. Kmt5b/c$^{-/-}$ double knockout mice also experience perinatal lethality (52). Kmt5b/c$^{-/-}$ null MEFs show decreased cell cycle progression, increased sensitivity to DNA damaging agents, altered chromatin structure and increased chromosomal aberrations, indicating that Kmt5b/c plays an important role in maintaining genome stability.

MMSET

Recent studies have also implicated the MMSET (Multiple Myeloma SET Domain Containing Protein) HMT in H4K20 dimethylation. HeLa cells depleted of MMSET lack H4K20me2 enrichment at DSBs. Additionally, 53BP1 foci formation is impaired in these cells (48,54). MMSET is known to bind to γH2AX and MDC1 in order to localize to damage sites (48). Multiple groups have since brought to light more evidence that KMT5B/C are primarily responsible for H4K20 dimethylation and 53BP1 foci formation

(53,55). It remains possible that both MMSET and KMT5B/C catalyze H4K20 dimethylation under different cellular conditions: KMT5B/C is likely to be responsible for the bulk of genome wide H4K20me2 while MMSET may be responsible for localized enrichment of H4K20me2 at DSBs.

H4K20me2 Binding Proteins

53BP1

There are multiple proteins known to bind to H4K20me2. 53BP1 is one of these chromatin readers (56). 53BP1 is a large protein, which is known to promote NHEJ of DSBs. The balance between 53BP1 and BRCA1 dictates NHEJ vs HR during S and G2 phases, and evidence shows that 53BP1 must be removed from DSBs in order to HR to proceed. This is facilitated by the chromatin remodeler SMARCAD1 (SWI/SNF-related matrix-associated actin-dependent regulator of chromatin subfamily A containing DEAD/H box 1) (see H2AK127ub section) (57). 53BP1 first recognizes γH2AX via its BRCT domains, and then subsequently binds to H4K20me2 using its tandem tudor domains, which are comprised of β-sheet folds (58-62). The binding affinities of the 53BP1 tandem tudor domains for H4K20me2 and H4K20me1 are 19.7 and 52.9 μM, respectively. They show an affinity of >1mM for unmodified and trimethylated H4K20. Disruption of the 53BP1 tandem tudor domains results in loss of H4K20me2 binding and loss of 53BP1 foci formation (56). 53BP1 also contains a UDR (ubiquitination-dependent recruitment motif), which mediates binding to H2AK15ub (see below) (63). Importantly, disruption of the 53BP1 UDR also results in loss of 53BP1 foci formation and impaired NHEJ (63) (Figure 2A).

Figure 2. 53BP1 recruitment to DNA DSB breaks. Upon damage, KMT5B/C methylate H4K20me1, forming H4K20me2. 53BP1 recognizes H4K20me2 *via* its tandem tudor domains. Additionally, RNF8 and RNF168 facilitate the ubiquitination of H2AK15. 53BP1 recognizes H2AK15ub *via* its UDR domain. 53BP1 is a bivalent reader of modified histones (A). Prior to damage, existing molecules of H4K20me2 are occupied by L3MBTL1 (B) and JMJD2A (C), which recognize H4K20me2 *via* their MBT and tudor domains, respectively. Upon DNA damage, RNF168 polyubiquitinates L3MBTL1 and JMJD2A, and VCP facilitates its removal and subsequent degradation by the proteasome. This leaves free H4K20me2, which can be recognized by 53BP1.

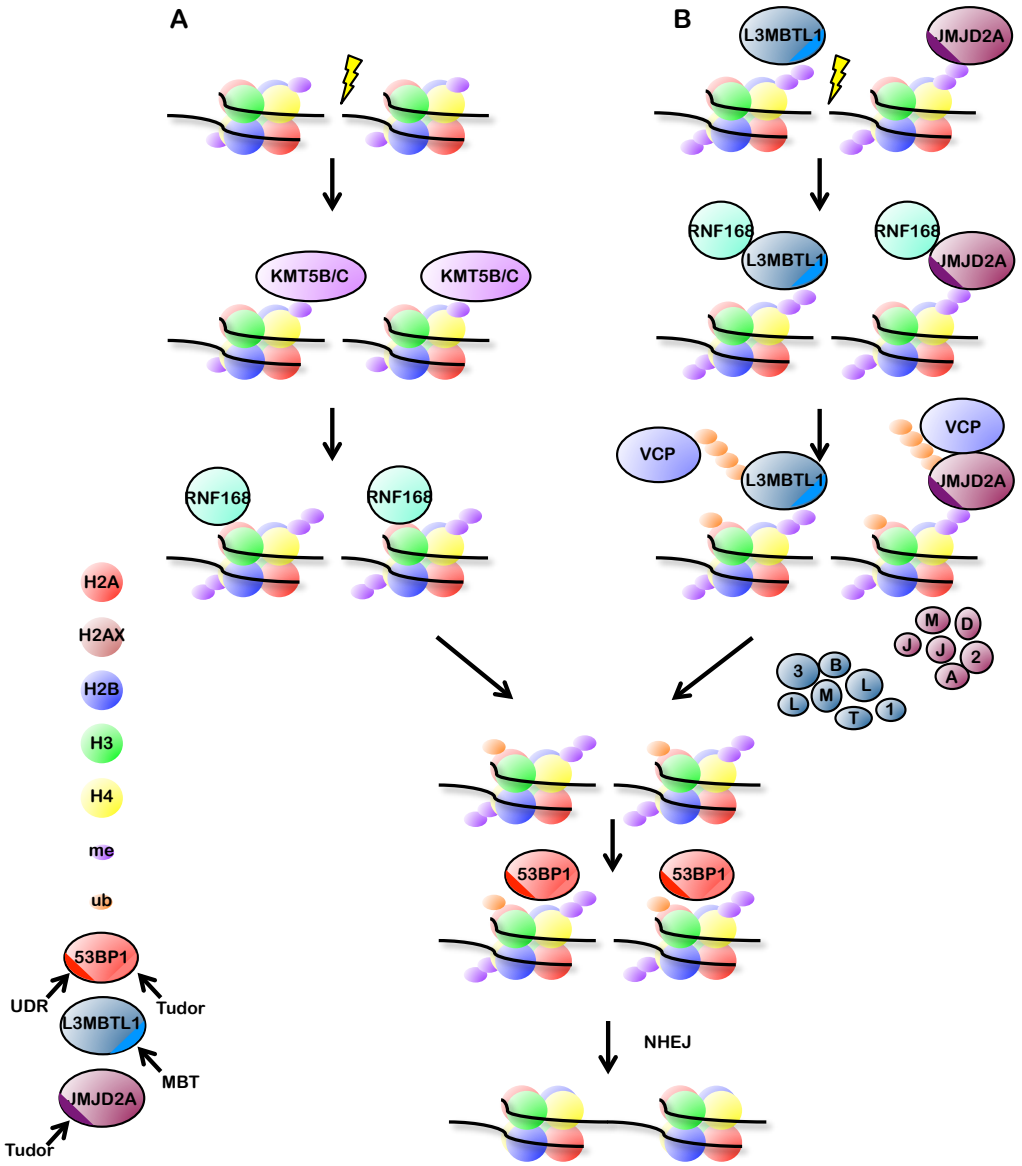
A
B
L3MBTL1
JMJD2A
KMT5B/C
KMT5B/C
RNF168
L3MBTL1
RNF168
JMJD2A
RNF168
RNF168
VCP
L3MBTL1
VCP
JMJD2A
H2A
H2AX
H2B
H3
H4
me
ub
53BP1
UDR
Tudor
L3MBTL1
MBT
JMJD2A
Tudor
53BP1
53BP1
NHEJ

Figure 2

JMJD2A

JMJD2A (Jumonji domain-containing protein 2A) also binds to H4K20me2 *via* its tandem tudor domains, although its specific function in binding H4K20me2 remains unknown. JMJD2A is a histone demethylase with specificity for H3K9me2/3 and H3K36me2/3(64). Upon DNA damage, JMJD2A is ubiquitinated by RNF8 (RING finger protein 8) and RNF168 (RING finger protein 168), and then degraded in a VCP (Valosin-containing protein) dependent manner. Removal of JMJD2A from H4K20me2 results in the subsequent recruitment of 53BP1(65). These findings indicate that DNA damage leads to both *de novo* H4K20me2 synthesis as well as the unmasking of this mark. The tudor domains of JMJD2A bind to H4K20me2 with a K_D of 2.0 μM, which represents an ~10-fold increased affinity over 53BP1, at least *in vitro*. Additionally, overexpression of JMJD2A abrogates 53BP1 foci formation, while knockdown of JMJD2A rescues 53BP1 foci formation in RNF8- and RNF168-depleted cells (65). These data suggest that JMJD2A may outcompete 53BP1 for H4K20me2 occupancy and must be removed in order for 53BP1 to bind. This same study demonstrated that the catalytic JmjC (Jumonji C) domain of JMJD2A is not required for blocking 53BP1 recruitment, indicating that 53BP1 recruitment is not dependent on JMJD2A demethylase activity (65) (Figure 2C).

L3MBTL1

L3MBTL1 (Lethal (3) malignant brain tumor-like protein 1) binds to H4K20me1 and H4K20me2 *via* its triple MBT (malignant brain tumor) domains in order to condense chromatin and repress transcription (66). Upon exposure to ionizing radiation, one study found as much as a 40% decrease in L3MBTL1 signal at DSBs. It was found that RNF8

and RNF168 ligase activity was indispensible for this reduction (67). While L3MBTL1 was shown to be ubiquitinated, it has yet to be determined if it is a substrate of RNF8 and RNF168. Acs et al. also found that L3MBTL1 is also degraded *via* VCP, and that L3MBTL1 ubiquitination and VCP catalytic activity are both required for reduction of L3MBTL1 DSB localization. Finally they showed that VCP is required for 53BP1 foci formation, and that RNF8 and RNF168 are required for VCP activity. They suggest that L3MBTL1 must be removed *via* VCP from H4K20me2 in order for 53BP1 to bind (67) (Figure 2C). Further studies into the relationship between 53BP1, L3MBTL1, and H4K20me2 are required to determine if 53BP1 binding to H4K20me2 is dependent on removal of L3MBTL1.

MBTD1

MBTD1 (malignant brain tumor domain-containing protein 1) binds to H4K20me2 *via* its four-MBT repeat domain (68,69). MBTD1 was recently identified as a component of the NuA4 chromatin-remodeling complex, which contains the histone acetyltransferase TIP60 (60 kDa Tat-interactive protein). Depletion of MBTD1 using siRNA results in persistent γH2AX foci formation following exposure to DNA damaging agents, indicating that MBTD1 is required for the timely repair of DNA damage. Additionally, depletion of MBTD1 leads to compromised HR and increased NHEJ. *In vitro* studies showed that MBTD1 can outcompete 53BP1 for H4K20me2 binding (70). *In* vivo, depletion of MBTD1 leads to persistent 53BP1 foci formation, attributed to inefficient removal of 53BP1 after damage. This group also found that TIP60 is responsible for

Figure 3. TIP60 recruitment to H4K20me2 and H2AK15 acetylation. Upon damage, KMT5B/C again catalyze H4K20 dimethylation. MBTD1 recognizes H4K20me2 *via* its MBT domains. As part of the NuA4/TIP60 complex, it recruits TIP60, which acetylates H2AK15. This acetylation blocks H2AK15 ubiquitination, and subsequent recognition by 53BP1 (A). After damage recognition, and H4K20 dimethylation by KMT5B/C, FANCD2 reads H4K20me2 *via* its MBD. TIP60 is recruited to FANCD2, where it acetylates H4K16. This blocks 53BP1 recognition of H4K20me2 and promotes HR (B).

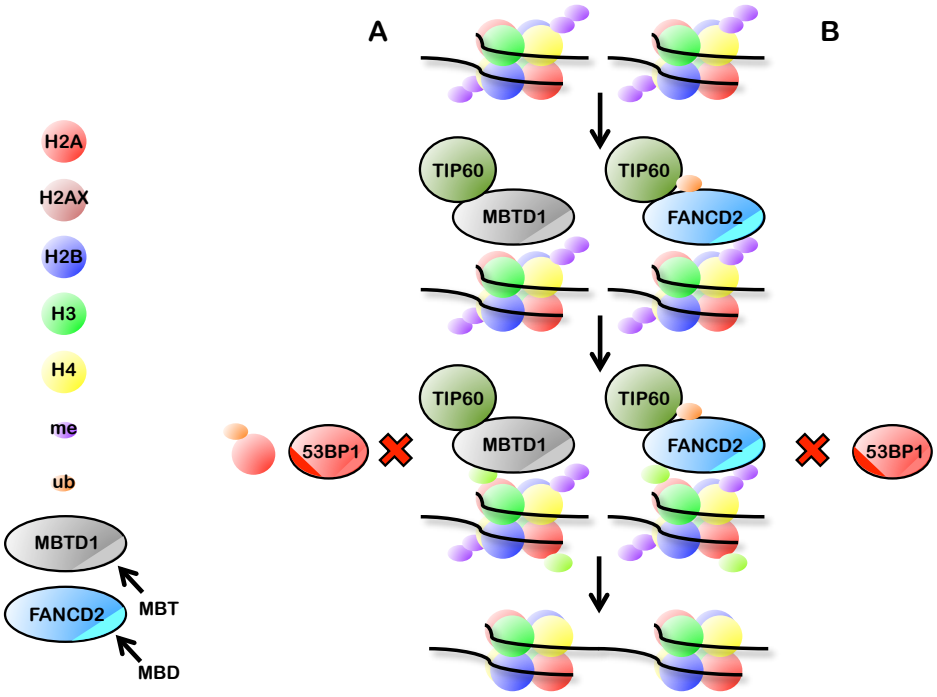
A
B
H2A
H2AX
H2B
H3
H4
me
ub
MBTD1
FANCD2
MBT
MBD
TIP60
MBTD1
TIP60
FANCD2
53BP1
53BP1

Figure 3

acetylating H2AK15 (see H2AK15ac section), which also impacts 53BP1 binding to H4K20me2, discussed in more detail below (70) (Figure 3A).

FANCD2

Our lab recently published findings that FANCD2 (Fanconi Anemia group D2) binds *in vitro* and *in vivo* to H4K20me2 *via* a methyl-binding domain. FANCD2 association with H4K20me2 increases in the presence of DNA damaging agents. FANCD2 is part of the Fanconi Anemia/Breast Cancer (FA/BRCA) DNA repair pathway, which removes interstrand crosslinks (ICLs) and promotes homologous recombination. Upon ICL damage, FANCD2 is monoubiquitinated and associates with chromatin and recruits HR repair proteins (71,72). FANCD2 has been shown to associate with the MRN complex *in vivo* and *in vitro*, and loss of any of the MRN complex members results in loss in FANCD2 foci formation (73). FANCD2 also relies on the presence of BRCA1 for foci formation (74,75). FANCD2 is required for CtIP localization to DSB sites, and its reduction results in reduced end resection and single strand DNA formation (76,77). FANCD2 monoubiquitination is also required for TIP60 recruitment, which acetylates in H4K16 (see H4K16ac section) (78,79) (Figure 3B). Finally, FANCD2 harbors a CUE (coupling of ubiquitin to ER degradation) domain, which binds to a currently unknown ubiquitin substrate. Mutation of this domain results in loss of FANCD2 chromatin localization, and increased cellular sensitivity to ICL-inducing agents (80). Disruption of the methyl-binding domain results in loss of FANCD2 foci formation, and increased 53BP1 chromatin and H4K20me2 association. FANCD2 promotes homologous recombination, and indeed, disruption of the methyl-binding domain leads to increased

NHEJ markers and chromosomal aberrations associated with loss of HR and repair via NHEJ.

ORC1

ORC1 (origin recognition complex subunit 1), while not a DNA repair protein, also associates with H4K20me2 *via* its BAH (bromo adjacent homology) domain. It was shown to preferentially bind to dimethylated H4K20 over the mono- or tri- methylated forms, and disruption of the BAH domain results in loss of H4K20me2 binding. ORC1 mediates replication licensing and forms a pre-replication complex alongside the MCM proteins. ORC1 BAH mutants also display decreased cell cycle progression, indicating that this domain is important of ORC1 function in replication. Disruption of the ORC1 BAH domain diminishes its ability to bind to chromatin at replication origins and affects cell cycle progression (81,82).

Histone Modifications that Impact Binding to H4K20me

H2AK15ub

As previously mentioned, 53BP1 not only binds to H4K20me2 *via* its tandem tudor domains, but also binds to H2AK15ub via its UDR. Disruption of the UDR results in loss of 53BP1 foci formation, indicating that both H4K20me2 and H2AK15ub are necessary for efficient 53BP1 recruitment (56,63). H2AK15 ubiquitination is catalyzed by RNF8 and RNF168, which are both required for 53BP1 accumulation at DNA damage sites (83-86). Following γH2AX and MDC1 foci formation, RNF8 recognizes MDC1 *via* its FHA domain, and then polyubiquitinates histone H1, a histone found within linker DNA

between nucleosomes (83,87). RNF168 then recognizes the K63-linked polyubiquitination of H1, and subsequently monoubiquitinates H2AK15 (84-87). Loss of RNF168 results in abrogation of 53BP1 foci formation. Recognition of both H2AK15ub and H4K20me2 by 53BP1 is necessary for efficient NHEJ. Interestingly, FAAP20, (Fanconi anemia core complex-associated protein 20) which promotes FANCD2 nuclear foci formation and HR, binds to Ub chains and requires RNF8 activity for its chromatin localization (88). However, the ubiquitinated substrate to which FAAP20 binds remains unknown (88,89). Finally, as previously touched upon, FANCD2 contains a CUE ubiquitin-binding domain and the ubiquitinated substrate to which it binds has yet to be determined (80). An intriguing possibility is that FANCD2 and 53BP1 may compete for bivalent recognition of both H4K20me2 and H2AK15ub.

H2AK15ac

H2A can be acetylated on lysine 15 (H2AK15ac) as well. The switch between H2AK15 ubiquitination and acetylation may regulate DNA repair pathway choice. Additionally, nucleosomes can be bivalently modified, so that H2AK15ac co-occur on nucleosomes containing H4K20me2. The NuA4/TIP60 complex acetylates H2AK15, precluding its ubiquitination, thereby preventing 53BP1 chromatin binding. As previously mentioned, MBTD1 recognizes H4K20me2 as part of the NuA4/TIP60 complex. Analysis of MBTD1 CRISPR/Cas9 knockout clones shows a modest reduction in H2AK15 acetylation, and MBTD1 overexpression slightly increases H2AK15ac levels, however the requirement of MBTD1 for H2AK15ac needs to be more closely examined. H2AK15ac appears most predominantly in G2/M phase, potentially overlapping with HR

in early G2, and continuing to evict 53BP1 throughout mitosis (70). In general, histone acetylation is downregulated after DNA damage, however H2AK15 acetylation was shown to increase after DNA damage, indicating the role of H2AK15 acetylation in DNA damage repair (70). While the authors suggest this mark is associated with HR, regulation of this mark and MBTD1 in pathway choice has yet to be studied.

H2AK127Ub

As mentioned above, upon damage recognition, MRN complex recruitment, and H2AX phosphorylation, CtIP is recruited to DSBs during homologous recombination in order to catalyze end resection. In BRCA1-deficient cells, 53BP1 blocks end resection, and NHEJ takes place. However, in BRCA1-proficient cells, HR is favorable during S-phase (33). BRCA1 recruits its heterodimeric binding partner, BARD1 (BRCA1- associated RING-domain protein), and unknown E2-ubiquitin conjugating enzyme(s), and then acts as an E3- ubiquitin conjugating enzyme to catalyze H2AK127 ubiquitination (90). SMARCAD1 (SWI/SNF-related matrix-associated actin-dependent regulator of chromatin subfamily A containing DEAD/H box 1), a member of the chromatin remodeling family of SWI/SNF proteins, then localizes to sites of damage. SMARACD1 contains a CUE ubiquitin-binding domain, and its chromatin recruitment is dependent on both its CUE domain and BARD1 expression. It was shown that the SMARCAD1 CUE domain can bind to H2A-ub fusion proteins *in vitro*, which suggests that SMARCAD1 is recruited to chromatin *via* its CUE domain binding to H2AK127ub. However this remains to clearly established. Upon SMARCAD1 recruitment, histone remodeling complexes reposition and evict nucleosomes, ultimately evicting 53BP1 from DNA

Figure 4. BRCA1-BARD1 and H2AK127 ubiquitination. Upon damage, BRCA1-BARD1 are recruited to DSB sites. Together they form an E3-ubiquitin ligase, and monoubiquitinate H2AK127. SMARCAD1, which is part of the SWI/SNF chromatin remodeling complex, recognizes H2AK127ub *via* its CUE ubiquitin binding domain. SWI/SNF remodels the chromatin, and evicts/blocks 53BP1 from H4K20me2 sites, promoting HR.

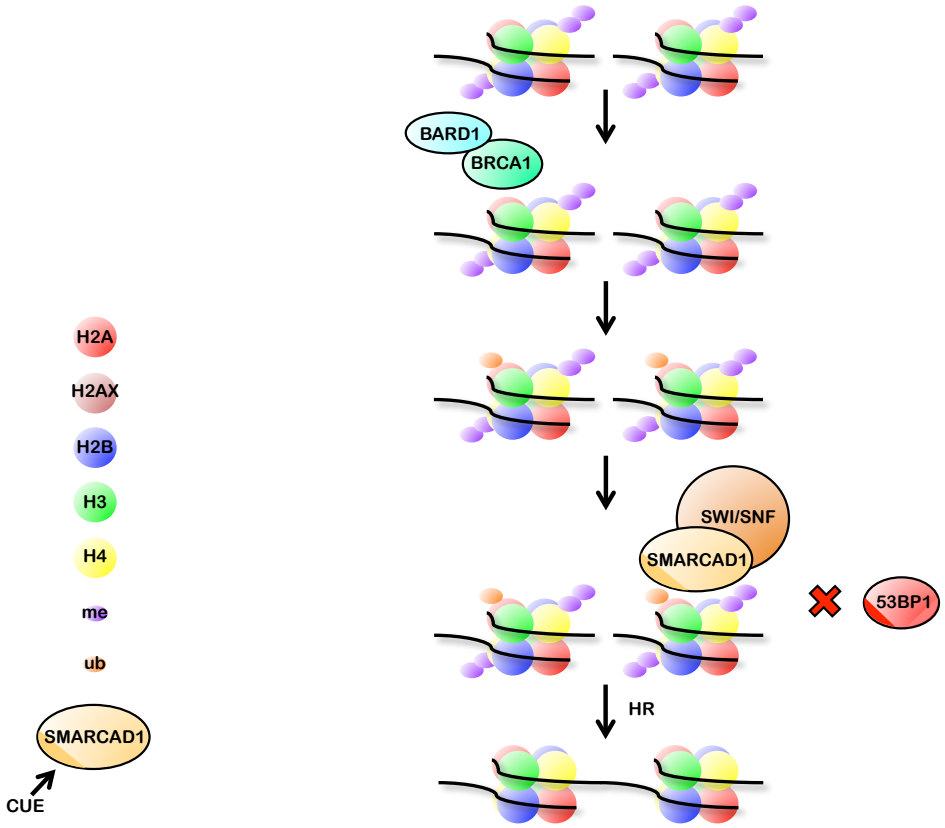
H2A
H2AX
H2B
H3
H4
me
ub
SMARCAD1
CUE
BARD1
BRCA1
SWI/SNF
SMARCAD1
53BP1
HR

Figure 4

damage sites. MRN and CtIP then promote end resection, and HR moves forward (57). This evidence is suggestive that SMARCAD1 binds to H2AK127Ub in order to reposition 53BP1, supporting previous work that shows that BRCA1 is involved in 53BP1 repositioning, and ultimate repair pathway choice (Figure 4). Much remains to be determined about the dynamics, regulation and molecular function of this particular chromatin mark.

H4K16ac

In addition to catalyzing H2AK15 acetylation, TIP60 also catalyzes the acetylation of H4K16 (91). In the absence of FANCD2, or more specifically FANCD2 monoubiquitination, TIP60 nuclear foci formation and overall levels of H4K16 acetylation are markedly reduced (79). *In vitro* binding experiments show that acetylation of K16 of a H4 peptide dimethylated at K20 results in decreased 53BP1 binding (53). *In vivo,* acetylation of H4K16 blocks 53BP1 recognition and chromatin recruitment (53,79,92). How H4K16 acetylation affects other H4K20me2 binding proteins such as MBTD1 and FANCD2 remains to be determined.

Conclusions

H4K20me2 joins a growing list of histone PTMs that play a major role in the coordination of DNA repair processes (Table 1). Until recently, γH2AX was one of the few posttranslationally modified histones with a well-characterized role in the DNA damage response. However, the importance of chromatin plasticity and, in particular,

histone PTMs for the orchestration of DNA repair has become increasingly well recognized. Many questions on the function and regulation of H4K20 methylation remain: For example, are the H4K20me *writers* and *erasers* differentially regulated in different tissue types? Do the different H4K20 methylation states have a role in the orchestration of loci-specific repair? In addition to H4K20 methylation, H3K9 and H3K27 methylation have also recently been shown to play key roles in the DNA damage response. Deciphering how the combinatorial modification of these marks and others coordinately contribute to DNA repair will be a considerable molecular challenge. While much remains to be answered, it is clear that the recognized roles for histone PTMs in the DNA damage response will continue to expand. As many of the *writers*, *erasers*, and *readers* of histone PTMs are druggable targets, a greater understanding of their homeostasis is highly likely to lead to the development of more targeted and effective combination cancer chemotherapy regimens.

Table 1. H4K20me2 binding proteins. Overview of proteins which bind to H4K20, and their roles in DNA damage repair.

Protein	Binding Partner	Role	Comments
KMT5A	H4K20	Writer	Methylates H4K20 to form H4K20me1
KMT5B/C	H4K20me	Writer	Methylates H4K20me1 to form H4K20me2/3
MMSET	H4K20me	Writer	Methylates H4K20me1 to form H4K20me2
53BP1	H4K20me2	Reader	Blocks CtIP and inhibits end resection; promotes NHEJ
	H2AK15ub		
JMJD2A	H4K20me2	Reader	Specific H4K20me2 binding function unknown; removed by VCP after DSB
L3MBTL1	H4K20me1/2	Reader	Binds to repress transcription; removed by VCP after DSB
MBTD1	H4K20me2	Reader	Part of NuA4/TIP60 complex, which acetylates H2AK15; promotes HR
FANCD2	H4K20me2	Reader	Recruits ICL repair proteins and TIP60; promotes HR
ORC1	H4K20me2	Reader	Mediates Replication Licensing
RNF8 and RNF 168	H2AK15	Writer	Monoubiquitinates H2AK15
	JMJD2A		Polyubiquitinates to signal removal of JMJD2A and L3MBTL1
	L3MBTL1		
BRCA1 and BARD1	H2AK127	Writer	Ubiquitinates H2AK127; read by SMARCAD1 and evicts 53BP1
TIP60	H4K16	Writer	Acetylates H4K16, blocking 53BP1 binding to H4K20me2

References:

1. Malik, H.S. and Henikoff, S. (2003) Phylogenomics of the nucleosome. *Nat Struct Biol*, **10**, 882-891.

2. West, M.H. and Bonner, W.M. (1980) Histone 2A, a heteromorphous family of eight protein species. *Biochemistry*, **19**, 3238-3245.

3. Miller, K.M. and Jackson, S.P. (2012) Histone marks: repairing DNA breaks within the context of chromatin. *Biochem Soc Trans*, **40**, 370-376.

4. Johnson, D.G. and Dent, S.Y. (2013) Chromatin: receiver and quarterback for cellular signals. *Cell*, **152**, 685-689.

5. Jackson, S.P. and Bartek, J. (2009) The DNA-damage response in human biology and disease. *Nature*, **461**, 1071-1078.

6. Uziel, T., Lerenthal, Y., Moyal, L., Andegeko, Y., Mittelman, L. and Shiloh, Y. (2003) Requirement of the MRN complex for ATM activation by DNA damage. *EMBO J*, **22**, 5612-5621.

7. Mirzoeva, O.K. and Petrini, J.H. (2001) DNA damage-dependent nuclear dynamics of the Mre11 complex. *Mol Cell Biol*, **21**, 281-288.

8. Rogakou, E.P., Pilch, D.R., Orr, A.H., Ivanova, V.S. and Bonner, W.M. (1998) DNA double-stranded breaks induce histone H2AX phosphorylation on serine 139. *J Biol Chem*, **273**, 5858-5868.

9. Burma, S., Chen, B.P., Murphy, M., Kurimasa, A. and Chen, D.J. (2001) ATM phosphorylates histone H2AX in response to DNA double-strand breaks. *J Biol Chem*, **276**, 42462-42467.

10. Stewart, G.S., Wang, B., Bignell, C.R., Taylor, A.M. and Elledge, S.J. (2003) MDC1 is a mediator of the mammalian DNA damage checkpoint. *Nature*, **421**, 961-966.

11. Lou, Z., Minter-Dykhouse, K., Franco, S., Gostissa, M., Rivera, M.A., Celeste, A., Manis, J.P., van Deursen, J., Nussenzweig, A., Paull, T.T. *et al.* (2006) MDC1 maintains genomic stability by participating in the amplification of ATM-dependent DNA damage signals. *Mol Cell*, **21**, 187-200.

12. Rogakou, E.P., Boon, C., Redon, C. and Bonner, W.M. (1999) Megabase chromatin domains involved in DNA double-strand breaks in vivo. *J Cell Biol*, **146**, 905-916.

13. Moynahan, M.E. and Jasin, M. (2010) Mitotic homologous recombination maintains genomic stability and suppresses tumorigenesis. *Nat Rev Mol Cell Biol*, **11**, 196-207.

14. Bressan, D.A., Baxter, B.K. and Petrini, J.H. (1999) The Mre11-Rad50-Xrs2 protein complex facilitates homologous recombination-based double-strand break repair in Saccharomyces cerevisiae. *Mol Cell Biol*, **19**, 7681-7687.

15. Taylor, E.M., Cecillon, S.M., Bonis, A., Chapman, J.R., Povirk, L.F. and Lindsay, H.D. (2010) The Mre11/Rad50/Nbs1 complex functions in resection-based DNA end joining in Xenopus laevis. *Nucleic Acids Res*, **38**, 441-454.

16. Mimitou, E.P. and Symington, L.S. (2010) Ku prevents Exo1 and Sgs1-dependent resection of DNA ends in the absence of a functional MRX complex or Sae2. *EMBO J*, **29**, 3358-3369.

17. Keelagher, R.E., Cotton, V.E., Goldman, A.S. and Borts, R.H. (2011) Separable roles for Exonuclease I in meiotic DNA double-strand break repair. *DNA Repair (Amst)*, **10**, 126-137.

18. Nimonkar, A.V., Genschel, J., Kinoshita, E., Polaczek, P., Campbell, J.L., Wyman, C., Modrich, P. and Kowalczykowski, S.C. (2011) BLM-DNA2-RPA-MRN and EXO1-BLM-RPA-MRN constitute two DNA end resection machineries for human DNA break repair. *Genes Dev*, **25**, 350-362.

19. Sugiyama, T., Zaitseva, E.M. and Kowalczykowski, S.C. (1997) A single-stranded DNA-binding protein is needed for efficient presynaptic complex formation by the Saccharomyces cerevisiae Rad51 protein. *J Biol Chem*, **272**, 7940-7945.

20. Ma, C.J., Gibb, B., Kwon, Y., Sung, P. and Greene, E.C. (2017) Protein dynamics of human RPA and RAD51 on ssDNA during assembly and disassembly of the RAD51 filament. *Nucleic Acids Res*, **45**, 749-761.

21. McIlwraith, M.J., Van Dyck, E., Masson, J.Y., Stasiak, A.Z., Stasiak, A. and West, S.C. (2000) Reconstitution of the strand invasion step of double-strand break repair using human Rad51 Rad52 and RPA proteins. *J Mol Biol*, **304**, 151-164.

22. Modesti, M., Budzowska, M., Baldeyron, C., Demmers, J.A., Ghirlando, R. and Kanaar, R. (2007) RAD51AP1 is a structure-specific DNA binding protein that stimulates joint molecule formation during RAD51-mediated homologous recombination. *Mol Cell*, **28**, 468-481.

23. Yuan, S.S., Lee, S.Y., Chen, G., Song, M., Tomlinson, G.E. and Lee, E.Y. (1999) BRCA2 is required for ionizing radiation-induced assembly of Rad51 complex in vivo. *Cancer Res*, **59**, 3547-3551.

24. Iwabuchi, K., Basu, B.P., Kysela, B., Kurihara, T., Shibata, M., Guan, D., Cao, Y., Hamada, T., Imamura, K., Jeggo, P.A. *et al.* (2003) Potential role for 53BP1 in DNA end-joining repair through direct interaction with DNA. *J Biol Chem*, **278**, 36487-36495.

25. Bunting, S.F., Callén, E., Wong, N., Chen, H.T., Polato, F., Gunn, A., Bothmer, A., Feldhahn, N., Fernandez-Capetillo, O., Cao, L. *et al.* (2010) 53BP1 inhibits homologous recombination in Brca1-deficient cells by blocking resection of DNA breaks. *Cell*, **141**, 243-254.

26. Blier, P.R., Griffith, A.J., Craft, J. and Hardin, J.A. (1993) Binding of Ku protein to DNA. Measurement of affinity for ends and demonstration of binding to nicks. *J Biol Chem*, **268**, 7594-7601.

27. Gottlieb, T.M. and Jackson, S.P. (1993) The DNA-dependent protein kinase: requirement for DNA ends and association with Ku antigen. *Cell*, **72**, 131-142.

28. Kurimasa, A., Kumano, S., Boubnov, N.V., Story, M.D., Tung, C.S., Peterson, S.R. and Chen, D.J. (1999) Requirement for the kinase activity of human DNA-dependent protein kinase catalytic subunit in DNA strand break rejoining. *Mol Cell Biol*, **19**, 3877-3884.

29. Grawunder, U., Wilm, M., Wu, X., Kulesza, P., Wilson, T.E., Mann, M. and Lieber, M.R. (1997) Activity of DNA ligase IV stimulated by complex formation with XRCC4 protein in mammalian cells. *Nature*, **388**, 492-495.

30. Li, Z., Otevrel, T., Gao, Y., Cheng, H.L., Seed, B., Stamato, T.D., Taccioli, G.E. and Alt, F.W. (1995) The XRCC4 gene encodes a novel protein involved in DNA double-strand break repair and V(D)J recombination. *Cell*, **83**, 1079-1089.

31. Durdíková, K. and Chovanec, M. (2017) Regulation of non-homologous end joining via post-translational modifications of components of the ligation step. *Curr Genet*, **63**, 591-605.

32. Ghezraoui, H., Piganeau, M., Renouf, B., Renaud, J.B., Sallmyr, A., Ruis, B., Oh, S., Tomkinson, A.E., Hendrickson, E.A., Giovannangeli, C. *et al.* (2014) Chromosomal translocations in human cells are generated by canonical nonhomologous end-joining. *Mol Cell*, **55**, 829-842.

33. Shibata, A. (2017) Regulation of repair pathway choice at two-ended DNA double-strand breaks. *Mutat Res*.

34. Moynahan, M.E., Chiu, J.W., Koller, B.H. and Jasin, M. (1999) Brca1 controls homology-directed DNA repair. *Mol Cell*, **4**, 511-518.

35. Wu, H., Siarheyeva, A., Zeng, H., Lam, R., Dong, A., Wu, X.H., Li, Y., Schapira, M., Vedadi, M. and Min, J. (2013) Crystal structures of the human histone H4K20 methyltransferases SUV420H1 and SUV420H2. *FEBS Lett*, **587**, 3859-3868.

36. Southall, S.M., Cronin, N.B. and Wilson, J.R. (2014) A novel route to product specificity in the Suv4-20 family of histone H4K20 methyltransferases. *Nucleic Acids Res*, **42**, 661-671.

37. Weirich, S., Kudithipudi, S. and Jeltsch, A. (2016) Specificity of the SUV4-20H1 and SUV4-20H2 protein lysine methyltransferases and methylation of novel substrates. *J Mol Biol*, **428**, 2344-2358.

38. Girish, T.S., McGinty, R.K. and Tan, S. (2016) Multivalent Interactions by the Set8 Histone Methyltransferase With Its Nucleosome Substrate. *J Mol Biol*, **428**, 1531-1543.

39. Kalashnikova, A.A., Porter-Goff, M.E., Muthurajan, U.M., Luger, K. and Hansen, J.C. (2013) The role of the nucleosome acidic patch in modulating higher order chromatin structure. *J R Soc Interface*, **10**, 20121022.

40. Nishioka, K., Rice, J.C., Sarma, K., Erdjument-Bromage, H., Werner, J., Wang, Y., Chuikov, S., Valenzuela, P., Tempst, P., Steward, R. *et al.* (2002) PR-Set7 is a nucleosome-specific methyltransferase that modifies lysine 20 of histone H4 and is associated with silent chromatin. *Mol Cell*, **9**, 1201-1213.

41. Fang, J., Feng, Q., Ketel, C.S., Wang, H., Cao, R., Xia, L., Erdjument-Bromage, H., Tempst, P., Simon, J.A. and Zhang, Y. (2002) Purification and functional characterization of SET8, a nucleosomal histone H4-lysine 20-specific methyltransferase. *Curr Biol*, **12**, 1086-1099.

42. Oda, H., Okamoto, I., Murphy, N., Chu, J., Price, S.M., Shen, M.M., Torres-Padilla, M.E., Heard, E. and Reinberg, D. (2009) Monomethylation of histone H4-lysine 20 is involved in chromosome structure and stability and is essential for mouse development. *Mol Cell Biol*, **29**, 2278-2295.

43. Sakaguchi, A. and Steward, R. (2007) Aberrant monomethylation of histone H4 lysine 20 activates the DNA damage checkpoint in Drosophila melanogaster. *J Cell Biol*, **176**, 155-162.

44. Tuzon, C.T., Spektor, T., Kong, X., Congdon, L.M., Wu, S., Schotta, G., Yokomori, K. and Rice, J.C. (2014) Concerted activities of distinct H4K20 methyltransferases at DNA double-strand breaks regulate 53BP1 nucleation and NHEJ-directed repair. *Cell Rep*, **8**, 430-438.

45. Oda, H., Hübner, M.R., Beck, D.B., Vermeulen, M., Hurwitz, J., Spector, D.L. and Reinberg, D. (2010) Regulation of the histone H4 monomethylase PR-Set7 by CRL4(Cdt2)-mediated PCNA-dependent degradation during DNA damage. *Mol Cell*, **40**, 364-376.

46. Paulsen, R.D., Soni, D.V., Wollman, R., Hahn, A.T., Yee, M.C., Guan, A., Hesley, J.A., Miller, S.C., Cromwell, E.F., Solow-Cordero, D.E. *et al.* (2009) A genome-wide siRNA screen reveals diverse cellular processes and pathways that mediate genome stability. *Mol Cell*, **35**, 228-239.

47. Jørgensen, S., Elvers, I., Trelle, M.B., Menzel, T., Eskildsen, M., Jensen, O.N., Helleday, T., Helin, K. and Sørensen, C.S. (2007) The histone methyltransferase SET8 is required for S-phase progression. *J Cell Biol*, **179**, 1337-1345.

48. Pei, H., Zhang, L., Luo, K., Qin, Y., Chesi, M., Fei, F., Bergsagel, P.L., Wang, L., You, Z. and Lou, Z. (2011) MMSET regulates histone H4K20 methylation and 53BP1 accumulation at DNA damage sites. *Nature*, **470**, 124-128.

49. Schotta, G., Lachner, M., Sarma, K., Ebert, A., Sengupta, R., Reuter, G., Reinberg, D. and Jenuwein, T. (2004) A silencing pathway to induce H3-K9 and H4-K20 trimethylation at constitutive heterochromatin. *Genes Dev*, **18**, 1251-1262.

50. Yang, H., Pesavento, J.J., Starnes, T.W., Cryderman, D.E., Wallrath, L.L., Kelleher, N.L. and Mizzen, C.A. (2008) Preferential dimethylation of histone H4 lysine 20 by Suv4-20. *J Biol Chem*, **283**, 12085-12092.

51. Foreman, K.W., Brown, M., Park, F., Emtage, S., Harriss, J., Das, C., Zhu, L., Crew, A., Arnold, L., Shaaban, S. *et al.* (2011) Structural and functional profiling of the human histone methyltransferase SMYD3. *PLoS One*, **6**, e22290.

52. Schotta, G., Sengupta, R., Kubicek, S., Malin, S., Kauer, M., Callén, E., Celeste, A., Pagani, M., Opravil, S., De La Rosa-Velazquez, I.A. *et al.* (2008) A chromatin-wide transition to H4K20 monomethylation impairs genome integrity and programmed DNA rearrangements in the mouse. *Genes Dev*, **22**, 2048-2061.

53. Hsiao, K.Y. and Mizzen, C.A. (2013) Histone H4 deacetylation facilitates 53BP1 DNA damage signaling and double-strand break repair. *J Mol Cell Biol*, **5**, 157-165.

54. Pei, H., Wu, X., Liu, T., Yu, K., Jelinek, D.F. and Lou, Z. (2013) The histone methyltransferase MMSET regulates class switch recombination. *J Immunol*, **190**, 756-763.

55. Hartlerode, A.J., Guan, Y., Rajendran, A., Ura, K., Schotta, G., Xie, A., Shah, J.V. and Scully, R. (2012) Impact of histone H4 lysine 20 methylation on 53BP1 responses to chromosomal double strand breaks. *PLoS One*, **7**, e49211.

56. Botuyan, M.V., Lee, J., Ward, I.M., Kim, J.E., Thompson, J.R., Chen, J. and Mer, G. (2006) Structural basis for the methylation state-specific recognition of histone H4-K20 by 53BP1 and Crb2 in DNA repair. *Cell*, **127**, 1361-1373.

57. Densham, R.M., Garvin, A.J., Stone, H.R., Strachan, J., Baldock, R.A., Daza-Martin, M., Fletcher, A., Blair-Reid, S., Beesley, J., Johal, B. *et al.* (2016) Human BRCA1-BARD1 ubiquitin ligase activity counteracts chromatin barriers to DNA resection. *Nat Struct Mol Biol*, **23**, 647-655.

58. Callebaut, I. and Mornon, J.P. (1997) From BRCA1 to RAP1: a widespread BRCT module closely associated with DNA repair. *FEBS Lett*, **400**, 25-30.

59. Schultz, L.B., Chehab, N.H., Malikzay, A. and Halazonetis, T.D. (2000) p53 binding protein 1 (53BP1) is an early participant in the cellular response to DNA double-strand breaks. *J Cell Biol*, **151**, 1381-1390.

60. Rappold, I., Iwabuchi, K., Date, T. and Chen, J. (2001) Tumor suppressor p53 binding protein 1 (53BP1) is involved in DNA damage-signaling pathways. *J Cell Biol*, **153**, 613-620.

61. Morales, J.C., Xia, Z., Lu, T., Aldrich, M.B., Wang, B., Rosales, C., Kellems, R.E., Hittelman, W.N., Elledge, S.J. and Carpenter, P.B. (2003) Role for the BRCA1 C-terminal repeats (BRCT) protein 53BP1 in maintaining genomic stability. *J Biol Chem*, **278**, 14971-14977.

62. Charier, G., Couprie, J., Alpha-Bazin, B., Meyer, V., Quéméneur, E., Guérois, R., Callebaut, I., Gilquin, B. and Zinn-Justin, S. (2004) The Tudor tandem of 53BP1: a new structural motif involved in DNA and RG-rich peptide binding. *Structure*, **12**, 1551-1562.

63. Fradet-Turcotte, A., Canny, M.D., Escribano-Díaz, C., Orthwein, A., Leung, C.C., Huang, H., Landry, M.C., Kitevski-LeBlanc, J., Noordermeer, S.M., Sicheri, F. *et al.* (2013) 53BP1 is a reader of the DNA-damage-induced H2A Lys 15 ubiquitin mark. *Nature*, **499**, 50-54.

64. Ozboyaci, M., Gursoy, A., Erman, B. and Keskin, O. (2011) Molecular recognition of H3/H4 histone tails by the tudor domains of JMJD2A: a comparative molecular dynamics simulations study. *PLoS One*, **6**, e14765.

65. Mallette, F.A., Mattiroli, F., Cui, G., Young, L.C., Hendzel, M.J., Mer, G., Sixma, T.K. and Richard, S. (2012) RNF8- and RNF168-dependent degradation of

KDM4A/JMJD2A triggers 53BP1 recruitment to DNA damage sites. *EMBO J*, **31**, 1865-1878.

66. Min, J., Allali-Hassani, A., Nady, N., Qi, C., Ouyang, H., Liu, Y., MacKenzie, F., Vedadi, M. and Arrowsmith, C.H. (2007) L3MBTL1 recognition of mono- and dimethylated histones. *Nat Struct Mol Biol*, **14**, 1229-1230.

67. Acs, K., Luijsterburg, M.S., Ackermann, L., Salomons, F.A., Hoppe, T. and Dantuma, N.P. (2011) The AAA-ATPase VCP/p97 promotes 53BP1 recruitment by removing L3MBTL1 from DNA double-strand breaks. *Nat Struct Mol Biol*, **18**, 1345-1350.

68. Nady, N., Krichevsky, L., Zhong, N., Duan, S., Tempel, W., Amaya, M.F., Ravichandran, M. and Arrowsmith, C.H. (2012) Histone recognition by human malignant brain tumor domains. *J Mol Biol*, **423**, 702-718.

69. Eryilmaz, J., Pan, P., Amaya, M.F., Allali-Hassani, A., Dong, A., Adams-Cioaba, M.A., Mackenzie, F., Vedadi, M. and Min, J. (2009) Structural studies of a four-MBT repeat protein MBTD1. *PLoS One*, **4**, e7274.

70. Jacquet, K., Fradet-Turcotte, A., Avvakumov, N., Lambert, J.P., Roques, C., Pandita, R.K., Paquet, E., Herst, P., Gingras, A.C., Pandita, T.K. *et al.* (2016) The TIP60 Complex Regulates Bivalent Chromatin Recognition by 53BP1 through Direct H4K20me Binding and H2AK15 Acetylation. *Mol Cell*, **62**, 409-421.

71. Garcia-Higuera, I., Taniguchi, T., Ganesan, S., Meyn, M.S., Timmers, C., Hejna, J., Grompe, M. and D'Andrea, A.D. (2001) Interaction of the Fanconi anemia proteins and BRCA1 in a common pathway. *Mol Cell*, **7**, 249-262.

72. Taniguchi, T., Garcia-Higuera, I., Andreassen, P.R., Gregory, R.C., Grompe, M. and D'Andrea, A.D. (2002) S-phase-specific interaction of the Fanconi anemia protein, FANCD2, with BRCA1 and RAD51. *Blood*, **100**, 2414-2420.

73. Roques, C., Coulombe, Y., Delannoy, M., Vignard, J., Grossi, S., Brodeur, I., Rodrigue, A., Gautier, J., Stasiak, A.Z., Stasiak, A. *et al.* (2009) MRE11-RAD50-NBS1 is a critical regulator of FANCD2 stability and function during DNA double-strand break repair. *EMBO J*, **28**, 2400-2413.

74. Bunting, S.F., Callén, E., Kozak, M.L., Kim, J.M., Wong, N., López-Contreras, A.J., Ludwig, T., Baer, R., Faryabi, R.B., Malhowski, A. *et al.* (2012) BRCA1 functions independently of homologous recombination in DNA interstrand crosslink repair. *Mol Cell*, **46**, 125-135.

75. Bogliolo, M., Lyakhovich, A., Callén, E., Castellà, M., Cappelli, E., Ramírez, M.J., Creus, A., Marcos, R., Kalb, R., Neveling, K. *et al.* (2007) Histone H2AX and Fanconi anemia FANCD2 function in the same pathway to maintain chromosome stability. *EMBO J*, **26**, 1340-1351.

76. Murina, O., von Aesch, C., Karakus, U., Ferretti, L.P., Bolck, H.A., Hänggi, K. and Sartori, A.A. (2014) FANCD2 and CtIP cooperate to repair DNA interstrand crosslinks. *Cell Rep*, **7**, 1030-1038.

77. Yeo, J.E., Lee, E.H., Hendrickson, E.A. and Sobeck, A. (2014) CtIP mediates replication fork recovery in a FANCD2-regulated manner. *Hum Mol Genet*, **23**, 3695-3705.

78. Hejna, J., Holtorf, M., Hines, J., Mathewson, L., Hemphill, A., Al-Dhalimy, M., Olson, S.B. and Moses, R.E. (2008) Tip60 is required for DNA interstrand cross-link repair in the Fanconi anemia pathway. *J Biol Chem*, **283**, 9844-9851.

79. Renaud, E., Barascu, A. and Rosselli, F. (2016) Impaired TIP60-mediated H4K16 acetylation accounts for the aberrant chromatin accumulation of 53BP1 and RAP80 in Fanconi anemia pathway-deficient cells. *Nucleic Acids Res*, **44**, 648-656.

80. Rego, M.A., Kolling, F.W., Vuono, E.A., Mauro, M. and Howlett, N.G. (2012) Regulation of the Fanconi anemia pathway by a CUE ubiquitin-binding domain in the FANCD2 protein. *Blood*, **120**, 2109-2117.

81. Zhang, W., Sankaran, S., Gozani, O. and Song, J. (2015) A Meier-Gorlin syndrome mutation impairs the ORC1-nucleosome association. *ACS Chem Biol*, **10**, 1176-1180.

82. Kuo, A.J., Song, J., Cheung, P., Ishibe-Murakami, S., Yamazoe, S., Chen, J.K., Patel, D.J. and Gozani, O. (2012) The BAH domain of ORC1 links H4K20me2 to DNA replication licensing and Meier-Gorlin syndrome. *Nature*, **484**, 115-119.

83. Huen, M.S., Grant, R., Manke, I., Minn, K., Yu, X., Yaffe, M.B. and Chen, J. (2007) RNF8 transduces the DNA-damage signal via histone ubiquitylation and checkpoint protein assembly. *Cell*, **131**, 901-914.

84. Stewart, G.S., Panier, S., Townsend, K., Al-Hakim, A.K., Kolas, N.K., Miller, E.S., Nakada, S., Ylanko, J., Olivarius, S., Mendez, M. *et al.* (2009) The RIDDLE syndrome protein mediates a ubiquitin-dependent signaling cascade at sites of DNA damage. *Cell*, **136**, 420-434.

85. Mattiroli, F., Vissers, J.H., van Dijk, W.J., Ikpa, P., Citterio, E., Vermeulen, W., Marteijn, J.A. and Sixma, T.K. (2012) RNF168 ubiquitinates K13-15 on H2A/H2AX to drive DNA damage signaling. *Cell*, **150**, 1182-1195.

86. Gatti, M., Pinato, S., Maspero, E., Soffientini, P., Polo, S. and Penengo, L. (2012) A novel ubiquitin mark at the N-terminal tail of histone H2As targeted by RNF168 ubiquitin ligase. *Cell Cycle*, **11**, 2538-2544.

87. Thorslund, T., Ripplinger, A., Hoffmann, S., Wild, T., Uckelmann, M., Villumsen, B., Narita, T., Sixma, T.K., Choudhary, C., Bekker-Jensen, S. *et al.* (2015) Histone H1 couples initiation and amplification of ubiquitin signalling after DNA damage. *Nature*, **527**, 389-393.

88. Yan, Z., Guo, R., Paramasivam, M., Shen, W., Ling, C., Fox, D., Wang, Y., Oostra, A.B., Kuehl, J., Lee, D.Y. *et al.* (2012) A ubiquitin-binding protein, FAAP20, links RNF8-mediated ubiquitination to the Fanconi anemia DNA repair network. *Mol Cell*, **47**, 61-75.

89. Leung, J.W., Wang, Y., Fong, K.W., Huen, M.S., Li, L. and Chen, J. (2012) Fanconi anemia (FA) binding protein FAAP20 stabilizes FA complementation group A (FANCA) and participates in interstrand cross-link repair. *Proc Natl Acad Sci U S A*, **109**, 4491-4496.

90. Kalb, R., Mallery, D.L., Larkin, C., Huang, J.T. and Hiom, K. (2014) BRCA1 is a histone-H2A-specific ubiquitin ligase. *Cell Rep*, **8**, 999-1005.

91. Kimura, A. and Horikoshi, M. (1998) Tip60 acetylates six lysines of a specific class in core histones in vitro. *Genes Cells*, **3**, 789-800.

92. Tang, J., Cho, N.W., Cui, G., Manion, E.M., Shanbhag, N.M., Botuyan, M.V., Mer, G. and Greenberg, R.A. (2013) Acetylation limits 53BP1 association with damaged chromatin to promote homologous recombination. *Nat Struct Mol Biol*, **20**, 317-325.

Manuscript-II

Prepared for submission to Proceedings of the National Academy of Sciences of the United States of America

FANCD2 binding to H4K20me2 *via* a methyl-binding domain is essential for efficient DNA crosslink repair

Karissa L. Paquin[a], Nicholas E. Mamrak[a], Paul A. Azzinaro[a], Elizabeth A. Vuono[a], Kevin E. Lima[a], Jodi L. Camberg[a], and Niall G. Howlett[a,1]

[a]Department of Cell and Molecular Biology, University of Rhode Island, Kingston, Rhode Island, U.S.A

[1]Corresponding author: Niall G. Howlett Ph.D., 379 Center for Biotechnology and Life Sciences, 120 Flagg Road, Kingston, RI, USA, Tel.: +1 401 874 4306; Fax: +1 401 874 2065; *Email address*: **nhowlett@uri.edu**

Keywords: Fanconi anemia, chromatin, ubiquitination, methylation, DNA crosslink repair

Biological Sciences: Biochemistry

FANCD2 binding to H4K20me2 *via* a methyl-binding domain is essential for efficient DNA crosslink repair

Karissa L. Paquin[a], Nicholas E. Mamrak[a], Paul A. Azzinaro[a], Elizabeth A. Vuono[a], Kevin E. Lima[a], Jodi L. Camberg[a], and Niall G. Howlett[a,1]

[a]Department of Cell and Molecular Biology, University of Rhode Island, Kingston, Rhode Island, U.S.A

[1]Corresponding author: Niall G. Howlett Ph.D., 379 Center for Biotechnology and Life Sciences, 120 Flagg Road, Kingston, RI, USA, Tel.: +1 401 874 4306; Fax: +1 401 874 2065; *Email address*: **nhowlett@uri.edu**

Keywords: Fanconi anemia, chromatin, ubiquitination, methylation, DNA crosslink repair

Fanconi anemia (FA) is an inherited disease characterized by bone marrow failure and increased cancer risk. FA is caused by mutation of any one of 22 genes, and the FA proteins function cooperatively to repair DNA interstrand crosslinks (ICLs). A central step in the activation of the FA pathway is the monoubiquitination of the FANCD2 and FANCI proteins, which occurs within chromatin. How FANCD2 and FANCI are anchored to chromatin remains unknown. In this study, we identify and characterize a FANCD2 histone-binding domain (HBD) and embedded methylated lysine-binding domain (MBD) and demonstrate binding specificity for H4K20me2. Disruption of the HBD/MBD compromises FANCD2 chromatin binding and nuclear foci formation and its ability to promote error-free DNA interstrand crosslink repair, leading to increased error-prone repair and genome instability. Our study functionally describes the first FA protein chromatin *reader* domain and establishes an important link between this human genetic disease and chromatin plasticity.

Significance

Fanconi anemia (FA) is a genetic disease characterized by atypically early-onset bone marrow failure and cancer. FA has strong genetic and biochemical links to hereditary breast and ovarian cancer. The FA proteins function to repair DNA damage and maintain genome stability. The FANCD2 protein functions at a critical stage of the FA pathway and its posttranslational modification is defective in >90% of FA patients. However, the domain structure, function, and regulation of FANCD2 remain remarkably poorly characterized. In this study, we describe the discovery of a novel chromatin-binding mechanism for FANCD2: FANCD2 contains a methyl-lysine binding motif with

specificity for H4K20me2. Disruption of this motif compromises FANCD2 chromatin binding; leading to defective DNA repair and increased genome instability.

Nucleosomes, the fundamental unit of chromatin, play a dynamic and instructive role in many cellular processes, including transcription, replication, and DNA repair. One mechanism by which nucleosomes instruct DNA repair is *via* the posttranslational modification (PTM) of histone tails. These modifications modulate the strength of noncovalent interactions between histones and DNA, and serve as binding sites for chromatin-interacting proteins, also known as chromatin *readers*. Many important DNA repair proteins have been shown to harbor *reader* domains that are critical for their repair function, examples of which include the tandem Tudor domains of 53BP1 and the chromodomain of KAT5/TIP60 (1-3).

Fanconi Anemia (FA) is a genetic disease characterized by congenital abnormalities, progressive pediatric bone marrow failure, and heightened cancer risk in early adulthood (4). FA is caused by mutation of any one of 22 genes (5, 6). The FA proteins orchestrate the repair of DNA interstrand crosslinks (ICLs), lesions that block the replication and transcription machineries, and can lead to structural and numerical chromosome aberrations if repaired erroneously (7, 8). A central step in the activation of the FA pathway is the site-specific monoubiquitination of the FANCD2 and FANCI proteins, which occurs within chromatin (9-12). However, the mechanism(s) by which FANCD2 is tethered to chromatin, and whether FANCD2 displays specificity for particular histone PTMs, is unknown. Indeed, no *reader* domains have been identified for any of the FA proteins to date.

In this study, we describe the identification and characterization of a FANCD2 histone-binding domain (HBD) and embedded methyl-lysine-binding domain (MBD). We establish that the FANCD2 MBD can bind to mono-, di-, and tri-methylated H4K20 *in vitro*, and exhibits specificity for H4K20me2 *in cellula*. Knockdown of KMT5A, the histone methyltransferase responsible for H4K20 monomethylation, which primes H4K20 for subsequent di- and tri- methylation, results in decreased FANCD2 foci formation and increased sensitivity to the DNA interstrand crosslink (ICL) inducing agent mitomycin C (MMC). Guided by sequence conservation and *in silico* modeling, we generated several HBD/MBD missense variants and stably transduced FA-D2 (*FANCD2*$^{-/-}$) patient-derived cells. Our functional analyses reveal that disruption of the HBD/MBD compromises FANCD2 chromatin binding and nuclear foci formation and its ability to effectively promote ICL repair. Consequently, upon exposure to ICL-inducing agents, error-prone DNA repair pathways, including nonhomologous DNA end joining (NHEJ), are employed, resulting in increased cytotoxicity and chromosome structural aberrations. Our studies uncover a novel and key mechanism by which FANCD2 is anchored to chromatin and functionally link this important human genetic disease to chromatin plasticity.

Results

FANCD2 has a histone-binding domain and embedded methyl-lysine-binding domain. A BLASTp search using short fragments of human FANCD2 uncovered amino acid sequence homology between FANCD2 and the *Drosophila melanogaster* p55 protein, a histone H4 binding protein and component of the NuRD, NuRF, and CAF1

nucleosome remodeling complexes (13-16) (Fig. S1A). This region of FANCD2 is highly evolutionarily conserved among vertebrates (Fig. S1A). Using an *in silico* molecular modeling approach, the histone H4 tail from the p55-H4 structure (PDB ID: 3C9C) was docked into murine Fancd2 (PDB ID: 3S4W) using AutoDock Vina (17), illustrating favorable predicted binding energies between the H4 tail and the histone-binding domain (HBD) (Fig. S1B). Further examination of the FANCD2 HBD uncovered a highly conserved putative methyl-lysine (Kme)-binding domain (MBD) with sequence homology to the methyl-binding chromodomains of HP1α, TIP60, and CBX8 (Fig. 1A and B). A GST-tagged FANCD2-HBD/MBD fragment (amino acids 604-1194) was purified and, in a histone peptide array screen, bound to a H4 17-mer harboring unmodified, K20me1, K20me2, and K20me3 (data not shown). These findings were verified in an *in vitro* histone peptide pulldown assay (Fig. S1C and D). Using a similar approach, a smaller GST-tagged FANCD2-MBD fragment (amino acids 1069-1142) bound to H4K20me1, H4K20me2, and H4K20me3, but not unmodified H4 or H3K27me3 (Fig. 1D). MBD-Kme binding involves the docking of Kme into an aromatic cage and the formation of cation-π interactions with delocalized electrons of aromatic residues (18). Highly conserved aromatic amino acids within the FANCD2 Kme binding cage include F1073, W1075, and F1078 (Fig. S1E). Using calf thymus histones, we observed a modest decrease in binding of a MBD-W1075A fragment to H4K20me2 and me3, compared to the wild-type MBD (Fig. S1F). Finally, using proximity ligation assay (PLA), we observed preferential binding of FANCD2 to H4K20me2 in cells, and stimulation of H4K20me binding upon MMC exposure (Fig. 1E and S1G). Binding of 53BP1 to H4K20me was used as a positive control for our PLA assay (Fig. S1H). Taken

Fig. 1. FANCD2 contains a MBD that exhibits specificity for H4K20me2. (A) Schematic of the known FANCD2 domains: N, Nuclear localization signal (49); CUE, Coupling of ubiquitin conjugation to endoplasmic reticulum degradation (41); P, PCNA-interaction motif (PIP-box) (50); HBD, Histone binding domain (aa 604-1194); MBD, Methyl lysine-binding domain (aa 1069-1142); T, Tower domain (51). (B) Clustal omega multiple sequence alignment (MSA) of the FANCD2 MBD and known methyl lysine-binding chromodomains. Predicted key aromatic residues are indicated by an asterisk, W1075 in blue. (C) Clustal omega zoo MSA of the FANCD2 MBD illustrating strong evolutionary conservation. (D) Streptavidin sepharose pulldown of biotinylated histone peptides incubated with purified GST-MBD. (E) Quantification of proximity ligation assay (PLA) results with FANCD2 and H4K20me1, me2, me3, and H3K27me3 in U2OS cells. Nuclei with >20 PLA spots were considered positive. Experiments were performed three times with similar results. Error bars represent the standard errors of the means from three independent experiments. At least 300 nuclei were scored per biological replicate. *, $P < 0.05$; **, $P < 0.01$; ***, $P < 0.001$.

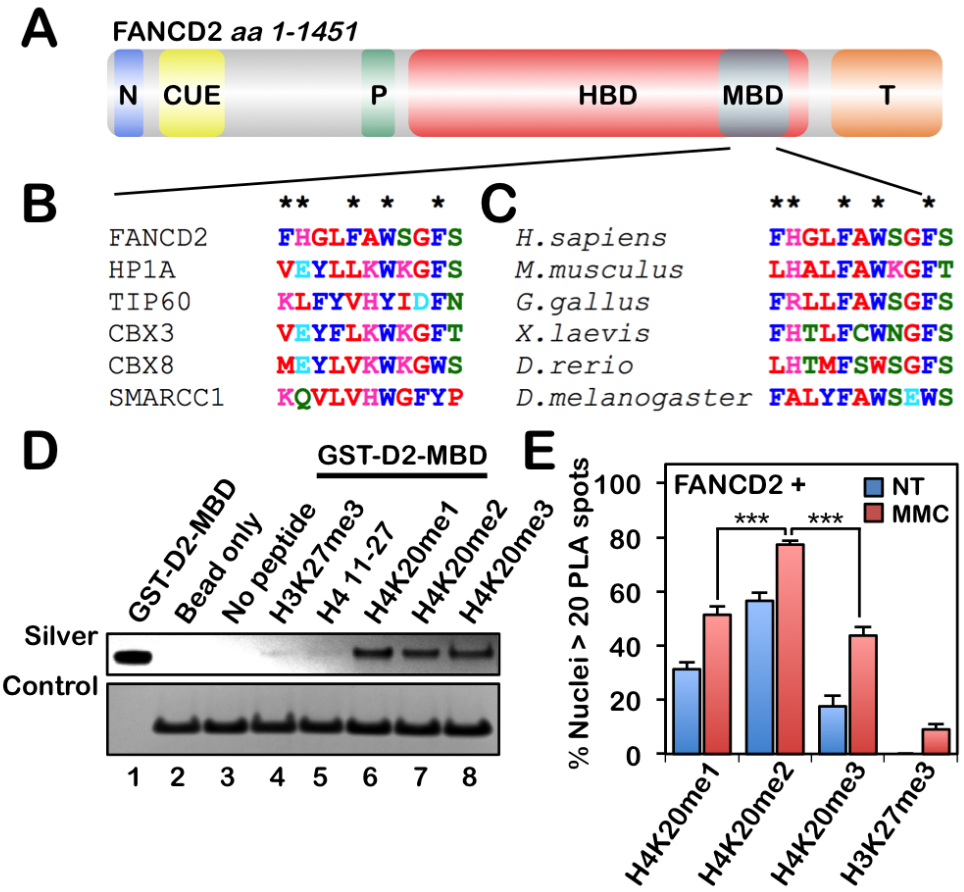
A
FANCD2 aa 1-1451
N
CUE
P
HBD
MBD
T
B
C
FANCD2 FHGLFAWSGFS
HP1A VEYLLKWKGFS
TIP60 KLFYVHYIDFN
CBX3 VEYFLKWKGFT
CBX8 MEYLVKWKGWS
SMARCC1 KQVLVHWGFYP
H.sapiens FHGLFAWSGFS
M.musculus LHALFAWKGFT
G.gallus FRLLFAWSGFS
X.laevis FHTLFCWNGFS
D.rerio LHTMFSWSGFS
D.melanogaster FALYFAWSEWS
D
GST-D2-MBD
GST-D2-MBD
Bead only
No peptide
H3K27me3
H4 11-27
H4K20me1
H4K20me2
H4K20me3
Silver
Control
1 2 3 4 5 6 7 8
E
FANCD2 +
NT
MMC
***
***
% Nuclei > 20 PLA spots
0
20
40
60
80
100
H4K20me1
H4K20me2
H4K20me3
H3K27me3

together, our results demonstrate that FANCD2 interacts directly with methylated H4 *via* its HBD/MBD, and suggest that the chromatin recruitment of FANCD2 is mediated *via* an interaction between the HBD/MBD and H4K20, similar to that recently described for other important DNA repair proteins, e.g. 53BP1 and TIP60 (1-3, 19).

The histone methyltransferase KMT5A is necessary for efficient activation of the FA pathway and ICL repair. The KMT5A histone methyltransferase catalyzes the monomethylation of H4K20, a prerequisite for di- and tri-methylation (20, 21). To determine if KMT5A plays a role in the regulation of the activation of the FA pathway, we depleted KMT5A in HeLa cells using siRNA and examined FANCD2 monoubiquitination and nuclear foci formation. While depletion of KMT5A did not impact spontaneous or DNA damage-inducible FANCD2 or FANCI monoubiquitination (Fig. 2A), KMT5A knockdown resulted in a significant decrease in FANCD2 nuclear foci formation following exposure to MMC and aphidicolin (APH), a replicative DNA polymerase inhibitor (Fig. 2B and C). Similar findings were observed for the nontransformed mammary epithelial line MCF10A (Fig. S2A and B). In addition, similar to FA patient-derived cells, cells depleted of KMT5A exhibited increased basal and ICL-inducible chromosome aberrations, including gaps, breaks and radial formations (Fig. 2D and E). These results establish that H4K20 methylation is necessary for efficient activation of the FA pathway and ICL repair.

The FANCD2 MBD is required for efficient chromatin binding and nuclear foci formation. To examine the functional importance of the FANCD2 HBD/MBD, we next

Fig. 2. The histone methyltransferase KMT5A is necessary for efficient activation of the FA pathway and ICL repair. (A) HeLa cells were incubated with control non-targeting siRNA (siControl) or siRNA targeting KMT5A (siKMT5A) for 72 h. Cells were then treated with 200 nM mitomycin C (MMC) or 1 μM aphidicolin (APH) for 16 h and whole-cell lysates analyzed by immunoblotting. L:S ratio, ratio of monoubiquitinated to nonubiquitinated FANCD2 or FANCI. (B) Representative images of FANCD2 foci in MMC-treated HeLa cells. Cells were treated as described in (A). D, DAPI; D2; FANCD2; M, merge. (C) Quantification of FANCD2 foci formation for (B). Nuclei with > 10 FANCD2 foci were considered positive. At least 300 nuclei were scored per biological replicate. (D) HeLa cells were incubated with siControl or siKMT5A for 72 h. Cells were then treated with 10 nM MMC for 16 h and metaphase chromosomes were analyzed for the presence of structural aberrations. 50 metaphases were scored per treatment. These experiments were performed twice with similar results. Error bars represent the standard errors of the means. *, $P < 0.05$; **, $P < 0.01$; ***, $P < 0.001$. (E) Representative chromosome images from (D). M, mitomycin C.

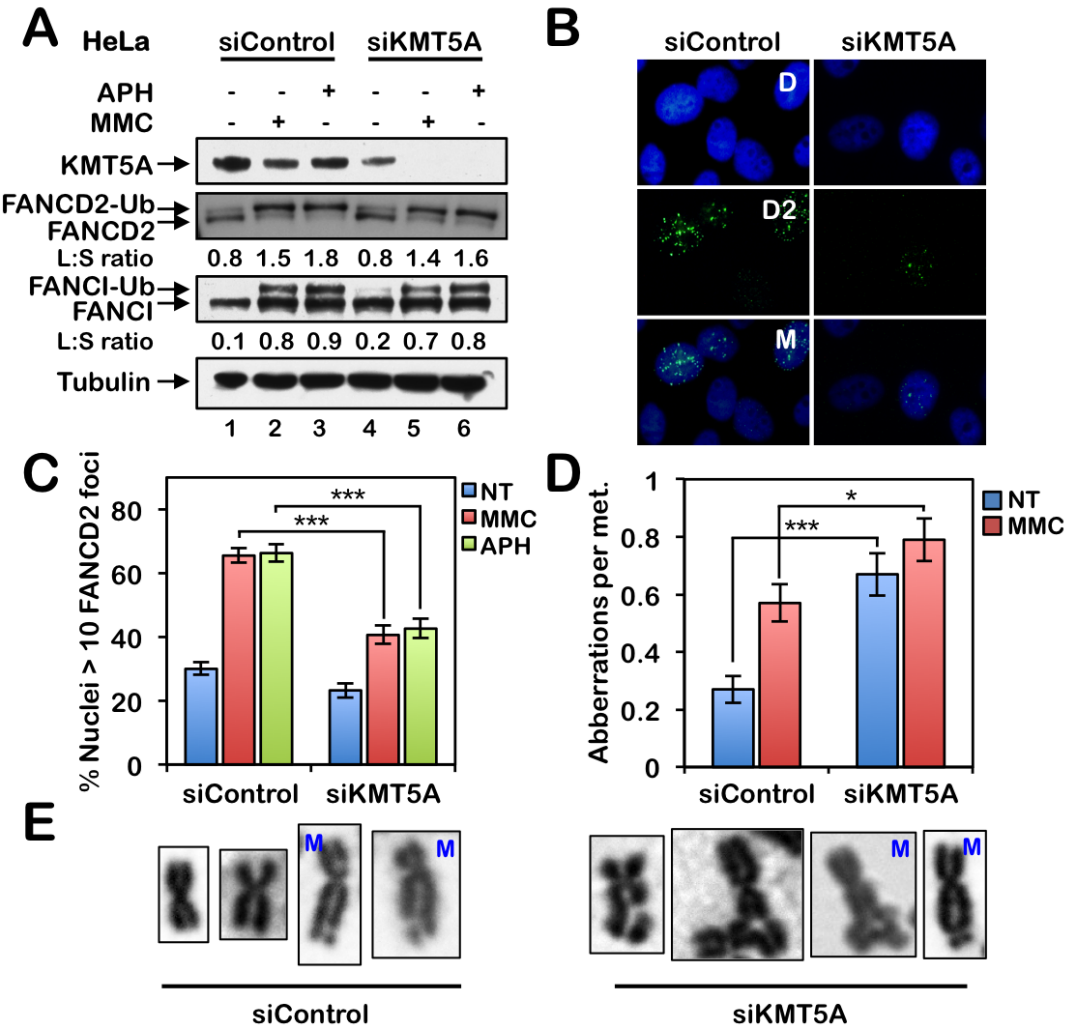
A
HeLa
siControl
siKMT5A
APH
MMC
KMT5A
FANCD2-Ub
FANCD2
L:S ratio
0.8 1.5 1.8 0.8 1.4 1.6
FANCI-Ub
FANCI
L:S ratio
0.1 0.8 0.9 0.2 0.7 0.8
Tubulin
1 2 3 4 5 6
B
siControl
siKMT5A
D
D2
M
C
% Nuclei > 10 FANCD2 foci
NT
MMC
APH
***
***
siControl
siKMT5A
D
Abberrations per met.
NT
MMC
*
***
siControl
siKMT5A
E
M
M
M
M
siControl
siKMT5A

generated a series of FANCD2 variants harboring missense mutations in the HBD/MBD, and stably expressed these mutants in FA-D2 (*FANCD2*$^{-/-}$) patient-derived cells (22). In contrast to the monoubiquitination-defective mutant FANCD2-K561R (10), all HBD/MBD missense mutants remained competent for DNA damage-inducible monoubiquitination (Fig. 3A). These findings indicate that mutations in the HBD/MBD do not perturb overall protein structure or stability, or the propensity for monoubiquitination by the multi-subunit FA core complex ubiquitin ligase. Using a chromatin enrichment assay, similar to wild type FANCD2, the HBD/MBD mutants were capable of localizing to chromatin (Fig. S3A). However, the interactions between the HBD/MBD mutants and chromatin were more sensitive to increasing salt concentrations than wild type FANCD2, leading to release of the mutants at lower salt concentrations (Fig. 3B and S3C). These results are suggestive of a reduced affinity of the mutants for chromatin. Moreover, similar to FANCD2-K561R and unlike wild type FANCD2, FANCD2-H1056A and FANCD2-W1075A failed to assemble into discrete nuclear foci following ICL exposure (Fig. 4A and C). Consistent with previous studies showing a dependency between FANCD2 and FANCI nuclear foci formation (11, 12), FANCI nuclear foci formation was also markedly impaired in cells expressing the HBD/MBD mutants (Fig. 4B). We next analyzed the interactions between FANCD2 and H4K20me in FA-D2 cells expressing wild type FANCD2 or the W1075A mutant using PLA. While wild type FANCD2 interacted strongly with H4K20me2 - and much less so with H4K20me1, H4K20me3, or H3K27me3 - this interaction was markedly impaired for the W1075A mutant (Fig. 4D). We simultaneously performed PLA with 53BP1 and H4K20me1, me2, me3, and H3K27me3 and observed a modest, yet statistically

Fig. 3. FANCD2 MBD mutants are proficient for monoubiquitination but exhibit decreased affinity for chromatin. (A) FA-D2 cells stably expressing LacZ, wild type FANCD2, FANCD2-K561R, FANCD2-H1056A, and FANCD2-W1075A were incubated in the absence or presence of 200 nM mitomycin C (MMC) or 200 μM hydroxyurea (HU) for 24 h, and whole-cell lysates were analyzed by immunoblotting. L:S ratio, ratio of monoubiquitinated to nonubiquitinated FANCD2 or FANCI. (B) FA-D2 cells stably expressing wild type FANCD2, FANCD2-H1056A, and FANCD2-W1075A were incubated in the absence or presence of 200 nM MMC for 24 h and nuclear fractions were extracted in buffers containing the indicated NaCl concentrations. Gels were stained with SimplyBlue SafeStain to confirm equal fraction loading.

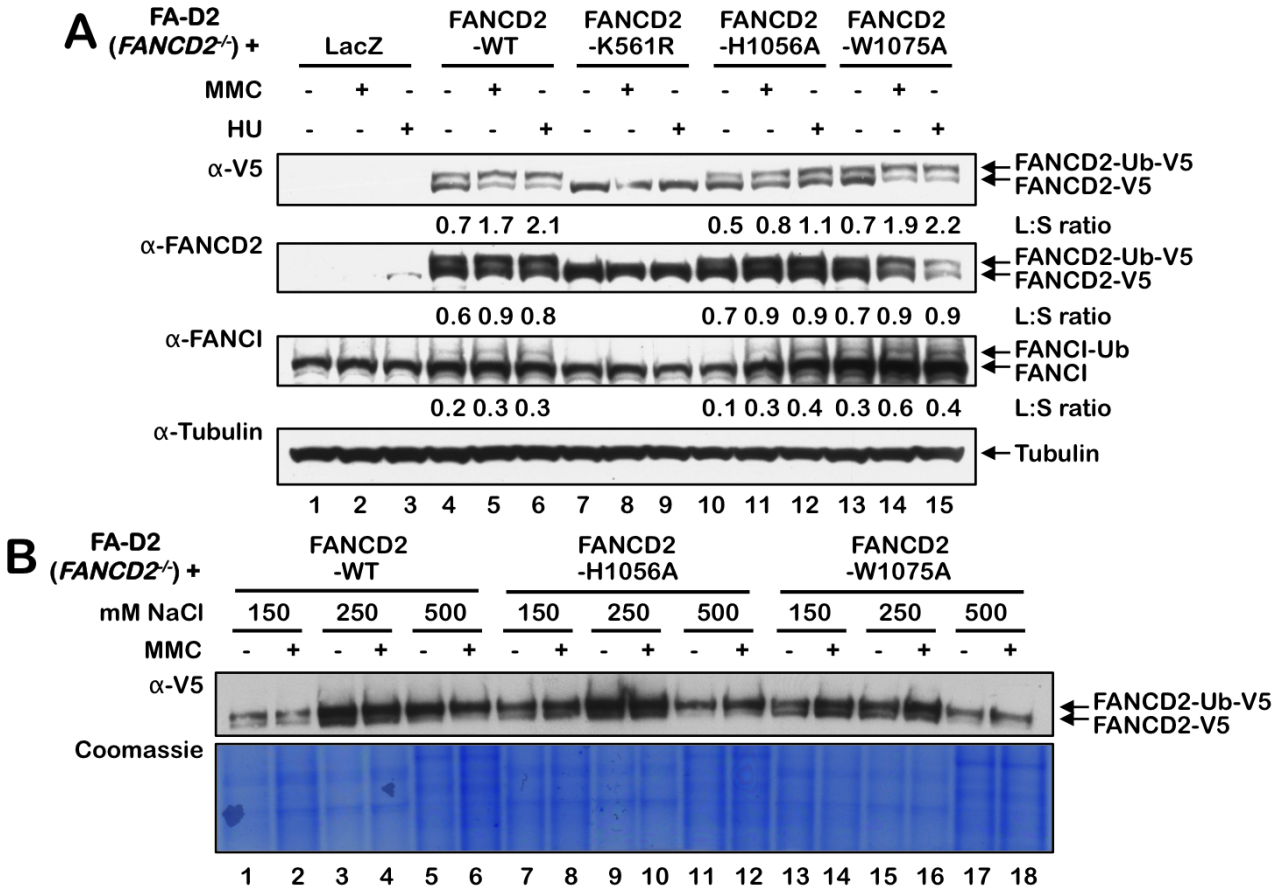
A
FA-D2 (FANCD2-/-) +
LacZ
FANCD2 -WT
FANCD2 -K561R
FANCD2 -H1056A
FANCD2 -W1075A
MMC
HU
α-V5
FANCD2-Ub-V5
FANCD2-V5
0.7 1.7 2.1 0.5 0.8 1.1 0.7 1.9 2.2
L:S ratio
α-FANCD2
FANCD2-Ub-V5
FANCD2-V5
0.6 0.9 0.8 0.7 0.9 0.9 0.7 0.9 0.9
L:S ratio
α-FANCI
FANCI-Ub
FANCI
0.2 0.3 0.3 0.1 0.3 0.4 0.3 0.6 0.4
L:S ratio
α-Tubulin
Tubulin
1 2 3 4 5 6 7 8 9 10 11 12 13 14 15
B
FA-D2 (FANCD2-/-) +
FANCD2 -WT
FANCD2 -H1056A
FANCD2 -W1075A
mM NaCl
150 250 500 150 250 500 150 250 500
MMC
α-V5
FANCD2-Ub-V5
FANCD2-V5
Coomassie
1 2 3 4 5 6 7 8 9 10 11 12 13 14 15 16 17 18

significant, increase in 53BP1 binding to H4K20me2 and me3 in FA-D2 cells expressing FANCD2-W1075A, compared to cells expressing wild type FANCD2 (Fig. S4). Taken together, our results indicate that FANCD2 preferentially binds to H4K20me2 in cells, and that binding is mediated by the HBD/MBD domain. In addition, our results suggest that decreased binding of H4K20me2 by FANCD2 may lead to increased H4K20me2 binding by 53BP1.

The FANCD2 HBD/MBD is required for efficient conservative ICL repair. To determine the impact of disruption of the HBD/MBD on ICL repair, we cultured cells in the absence and presence of MMC and examined γH2AX nuclear foci formation, a marker of DNA double-strand break (DSB) formation (23). Unlike FA-D2 cells expressing wild type FANCD2, cells expressing FANCD2-H1056A and -W1075A exhibited prolonged elevated γH2AX nuclear foci formation following ICL exposure (Fig. 5A). We also examined 53BP1 and DNA-PKcs pS2056 nuclear foci formation in our FA-D2 cell series, both markers of error-prone NHEJ DSB repair (24-27). Similar to that observed for γH2AX, persistent elevated levels of 53BP1 and DNA-PKcs pS2056 nuclear foci were observed in cells expressing FANCD2-H1056A and -W1075A, in contrast to cells expressing wild type FANCD2 (Fig. 5B and S5B). We also measured cell survival and metaphase chromosome aberrations in HBD/MBD mutant expressing cells. Similar to FANCD2-K561R, and unlike wild type FANCD2, the FANCD2-H1056A and -W1075A mutants failed to fully rescue the ICL sensitivity of FA-D2 patient cells (Fig. 5C). Chromosomes from cells expressing FANCD2-H1056A and -W1075A also exhibited greater numbers of aberrations, including gaps and breaks and

Fig. 4. FANCD2 MBD mutants fail to assemble into nuclear foci or interact with H4K20me2. (A and B) FA-D2 cells stably expressing wild type FANCD2, FANCD2-K561R, FANCD2-H1056A, and FANCD2-W1075A were incubated in the absence or presence of 200 nM mitomycin C (MMC) for 24 h. Cells were fixed and stained with anti-FANCI (green) and anti-V5 (red) antibodies and counterstained with DAPI (blue). (A) Quantification of FANCD2 nuclear foci. (B) Quantification of FANCI nuclear foci. Nuclei with >5 V5 (FANCD2) or FANCI foci were considered positive. (C) Representative images from (A) and (B). (D) Quantification of proximity ligation assay (PLA) results with FANCD2 and H4K20me1, me2, me3, and H3K27me3 in FA-D2 cells stably expressing wild type FANCD2 or FANCD2-W1075A. Nuclei with >20 PLA spots were considered positive. Experiments were performed three times with similar results. At least 300 nuclei were scored per biological replicate. Error bars represent the standard errors of the means from three independent experiments. *, $P < 0.05$; **, $P < 0.01$; ***, $P < 0.001$.

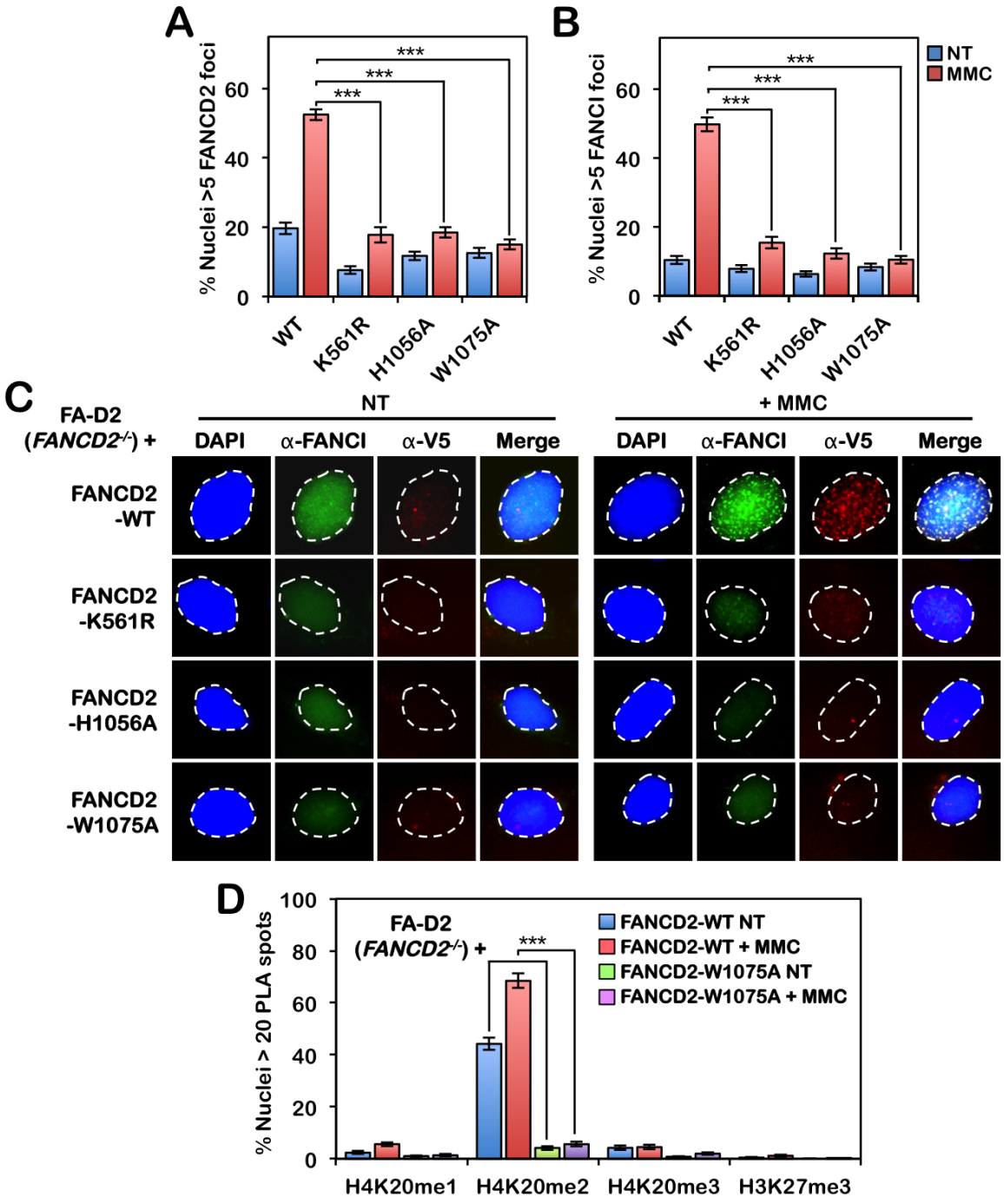
A
% Nuclei >5 FANCD2 foci
***
***
***
0
20
40
60
WT
K561R
H1056A
W1075A
B
% Nuclei >5 FANCI foci
NT
MMC
C
FA-D2
(FANCD2-/-) +
NT
+ MMC
DAPI
α-FANCI
α-V5
Merge
FANCD2
-WT
FANCD2
-K561R
FANCD2
-H1056A
FANCD2
-W1075A
D
% Nuclei > 20 PLA spots
FA-D2
(FANCD2-/-) +
FANCD2-WT NT
FANCD2-WT + MMC
FANCD2-W1075A NT
FANCD2-W1075A + MMC
0
20
40
60
80
100
H4K20me1
H4K20me2
H4K20me3
H3K27me3

radial formations, compared with cells expressing wild type FANCD2 (Fig. 5D and S5A). Stable expression of FANCD2-H1056A and -W1075A had no observable impact on cellular growth rate (Fig. S5C). Taken together, our findings indicate that H4K20me2 binding by the FANCD2 HBD/MBD is essential for the promotion of error-free conservative ICL repair, and link chromatin plasticity to activation of an important tumor suppressor pathway.

Discussion

In this study, we describe the identification and functional characterization of a methyl-lysine binding domain in the FANCD2 protein that exhibits specificity for H4K20me2. Disruption of this domain results in a decreased affinity for chromatin and an inability to assemble into discrete nuclear foci, presumed sites of active ICL repair (10). Consequently, cells expressing FANCD2 MBD mutants demonstrate evidence of persistent DSBs and an increased dependence on error-prone ICL repair pathways, including NHEJ. This, in turn, leads to increased sensitivity to ICL-inducible chromosome structural aberrations and cytotoxicity. A role for the FA proteins in suppressing erroneous NHEJ repair has previously been described (24). Consistent with an important role for the H4K20me2 chromatin mark in facilitating efficient activation of the FA pathway and ICL repair, depletion of the KMT5A H4K20 monomethyltransferase markedly reduced FANCD2 nuclear foci formation following ICL exposure. Mutation of the MBD and depletion of KMT5A did not, however, impact FANCD2 or FANCI monoubiquitination. This is consistent with several reports demonstrating the uncoupling of monoubiquitination from nuclear foci formation (10, 28-31). Collectively, these

Fig. 5. The FANCD2 HBD/MBD is required for efficient conservative ICL repair. (A and B) FA-D2 cells stably expressing LacZ, wild type FANCD2, FANCD2-K561R, FANCD2-H1056A, and FANCD2-W1075A were incubated in the absence or presence of 200 nM mitomycin C (MMC) for 24 h and allowed to recover for an additional 24 h. Cells were fixed and stained with anti-γH2AX (A) or anti-53BP1 (B) antibodies and the numbers of nuclei with >10 γH2AX (A) or >20 53BP1 (B) foci were scored. At least 300 nuclei were scored per biological replicate. (C) The same cells were incubated in the presence of various concentrations of MMC for 7-10 days and surviving cells were stained with crystal violet and % survival scored relative to untreated cells. (D) The same cells were incubated in the absence (NT) or presence of 16 nM MMC for 24 h and metaphase chromosomes analyzed for structural aberrations, including gaps, breaks and radial formations. Representative chromosome aberrations from MMC-treated FA-D2 cells expressing FANCD2-H1056A and FANCD2-W1075A are shown. All experiments were performed three times with similar results, except for (D), which was performed twice. Error bars represent the standard errors of the means. For (D), 80 metaphases were scored per treatment. *, $P < 0.05$; **, $P < 0.01$; **

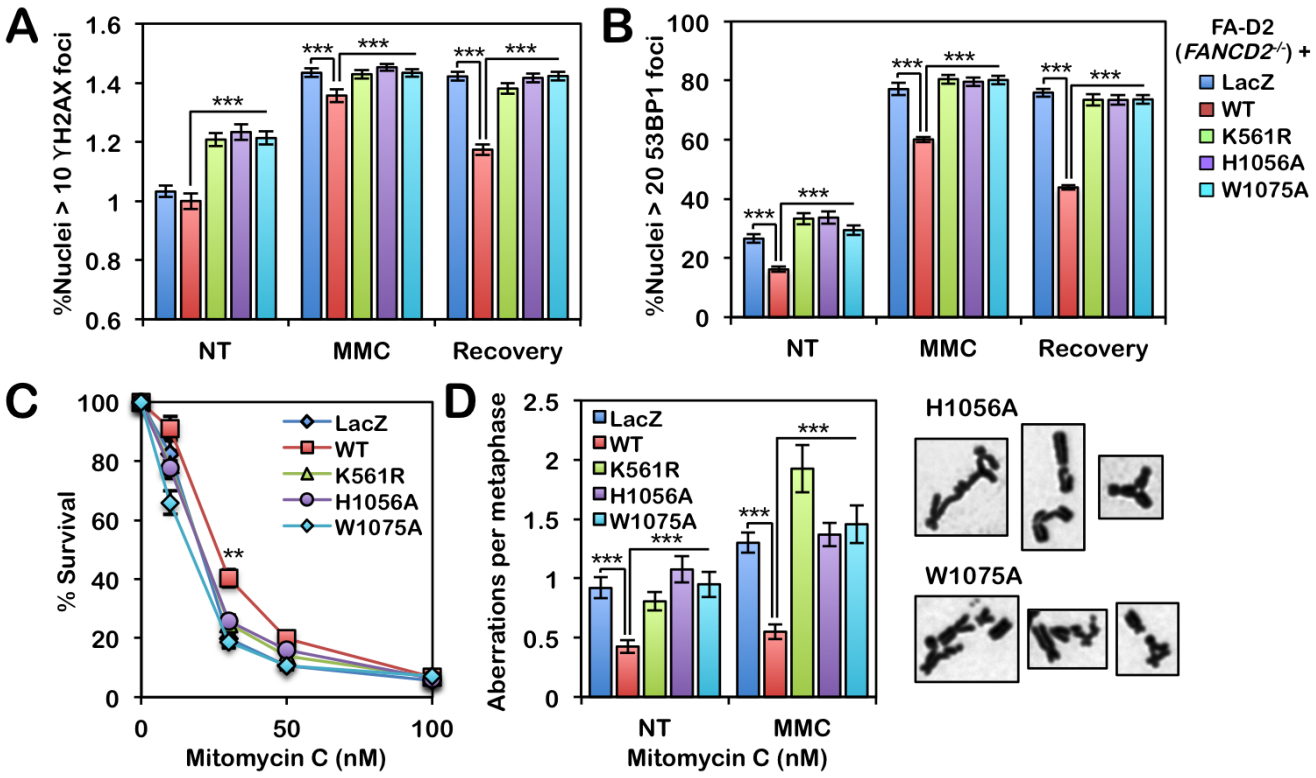
A
%Nuclei > 10 γH2AX foci
1.6
1.4
1.2
1
0.8
0.6
***
NT
MMC
Recovery
B
%Nuclei > 20 53BP1 foci
100
80
60
40
20
0
FA-D2 (FANCD2-/-) +
LacZ
WT
K561R
H1056A
W1075A
C
% Survival
100
80
60
40
20
0
**
0
50
100
Mitomycin C (nM)
D
Aberrations per metaphase
2.5
2
1.5
1
0.5
0
NT
MMC
Mitomycin C (nM)
H1056A
W1075A

studies indicate that monoubiquitination is necessary but not sufficient for nuclear foci formation, and that the ability of FANCD2 to assemble into nuclear foci is essential for effective ICL repair. Moreover, our findings indicate that one critical determinant of FANCD2 nuclear foci formation is the ability to interact directly with H4K20me2.

The importance of the H4K20me2 chromatin mark for efficient DNA repair has become increasingly well recognized (32). Loss of KMT5A (PR-SET7/SET8), or the KMT5B (SUV4-20H1) and KMT5C (SUV4-20H2) methyltransferases - which mediate di- and tri-methylation of H4K20 - results in widespread genome instability across the evolutionary spectrum (33-36). H4K20me2 has been shown to be an important factor for the chromatin recruitment of 53BP1. 53BP1 promotes NHEJ and suppresses homologous recombination (HR) by negatively regulating 5'-3' DNA strand resection, a critical initiating step of HR (25, 27). 53BP1 binds to H4K20me2 *via* its tandem Tudor domains (1). Similar to our findings for the FANCD2 MBD, disruption of the Tudor folds compromises the recruitment of 53BP1 to sites of DNA damage (37). However, while delayed, *Suv4-20h*-double-null MEFs support 53bp1 nuclear foci formation following exposure to ionizing radiation (IR) (36), highlighting the multifactorial nature of its chromatin recruitment. For example, binding to H2AK15ub *via* its ubiquitination-dependent recruitment motif (UDR) also promotes 53BP1 chromatin binding (38). Conversely, TIP60-mediated H2AK15 and H4K16 acetylation inhibits 53BP1 chromatin binding (39, 40). While much less is known about mechanistic aspects of FANCD2 chromatin recruitment, we predict a similar scenario with the existence of multiple determinants of chromatin targeting. Our studies indicate that FANCD2 binding to H4K20me2 is necessary for stable association and site-specific accumulation within

chromatin. We also previously established that FANCD2 has an ubiquitin-binding domain: an amino-terminal CUE (for coupling of ubiquitin conjugation to endoplasmic reticulum degradation) domain (41). While the CUE is required for efficient chromatin targeting, the ubiquitinated protein to which the CUE domain binds has yet to be identified. The RNF8 and BRCA1-BARD1 E3 ubiquitin ligases have also been shown to be required for the efficient chromatin recruitment of FANCD2 (10, 29, 42, 43), leading us to predict that FANCD2, like 53BP1, may also function as a bivalent chromatin reader. Interestingly, we observed a modest increase in 53BP1 binding to H4K20me2 upon mutation of the FANCD2 MBD, suggesting that FANCD2 and 53BP1 may compete for binding to the H4K20me2 mark. FANCD2 has been shown to promote the recruitment of TIP60 and the acetylation of H4K16 (44), which would be expected to decrease the affinity of 53BP1 for chromatin binding. The relationship between 53BP1 and FANCD2 remains to be clearly elucidated: while FANCD2 is generally thought to promote HR and restrict NHEJ (24, 45-47), combined deletion of murine *53bp1* and *Fancd2* results in increased ICL-inducible genomic instability compared to deletion of *Fancd2* alone (29). Studies of ICL repair using *Xenopus* egg extracts have established that FANCD2 is required for nucleolytic incisions proximal to the ICL (48), and the absence of FANCD2 may thus preclude the generation of an optimal initiating structure for both HR and NHEJ. Future studies of the interplay between FANCD2 and 53BP1, the chromatin modifications that dictate their functions, and the chromatin remodeling complexes with which they interact, will be essential for improving our understanding of ICL repair, the molecular basis of FA, and the development of effective therapeutic options for FA.

Materials and Methods

Cell Culture

FA-D2 (*FANCD2*$^{-/-}$) cells were grown in DMEM supplemented with 15% v/v fetal bovine serum, 1% v/v L-glutamine, and 1% v/v penicillin/streptomycin. Cells were stably infected with pLenti6.2/V5-DEST (Invitrogen) harboring wild type or mutant FANCD2 cDNAs. Stably infected cells were grown in DMEM complete medium supplemented with 2 μg/mL blasticidin.

NaCl Extraction

Cells were plated at a density of 3 x 10^6 cells in 15 cm^2 dishes. Cells were treated with 200 nM MMC for 24 h. Cells were harvested in ice-cold PBS, and a portion was set aside for the whole-cell lysate. The remaining pellet was lysed in CSK buffer and the supernatant containing soluble proteins was collected. The remaining pellet was split into three and lysed in salt extraction buffer (20 mM HEPES, pH 7.9, 0.5 mM TCEP, 1 mM PMSF, 1.5 mM $MgCl_2$, and 0.1% Triton-X-100) containing 150, 250, or 500 mM NaCl.

In vitro Histone Peptide Binding Assays

GST-fusion proteins were incubated with biotinylated histone peptides (Epicypher) overnight at 4°C overnight in Binding Buffer (50 mM Tris-HCl pH 7.5, 150 mM NaCl, 0.05% v/v NP-40). Samples were incubated for 1 h at 4°C with Streptavidin sepharose (GE) (previously washed in in Binding Buffer). After incubation, samples were washed

4x with Wash Buffer (50 mM Tris-HCl pH 7.5, 200 mM NaCl, 0.1% v/v NP-40) and eluted in 2x LDS/10% v/v β-mercaptoethanol with boiling. Proteins were resolved on 4-12% w/v Bis-Tris gels (Invitrogen), and either silverstained using the Silver Stain for Mass Spectrometry kit (Thermo), or immunoblotted with antibodies against GST (Invitrogen).

ACKNOWLEDGEMENTS

We thank members of the Howlett laboratory for critical reading of this manuscript and for helpful discussions. This work was supported by National Institutes of Health/National Heart, Lung and Blood Institute grant R01HL101977 (NGH); Rhode Island IDeA Network of Biomedical Research Excellence (RI-INBRE) grant P20GM103430 from the National Institute of General Medical Sciences; and Rhode Island Experimental Program to Stimulate Competitive Research (RI-EPSCoR) grant #1004057 from the National Science Foundation. KEL was the recipient of a University of Rhode Island Science & Engineering Summer Undergraduate Research Fellowship. NEM was the recipient of a RI-INBRE Summer Undergraduate Research Fellowship.

Author Contributions

KLP and NGH designed the experiments. KLP, PAA, EAV, KEL, AND NEM performed the experiments. KLP, PAA, and NGH analyzed the data. JLC provided advice on protein purifications and *in vitro* binding assays KLP and NGH wrote the manuscript.

Conflict of Interest

The author(s) declare no competing financial interests.

Supplemental Information

Supplemental Information includes five supplementary figures, materials and methods, and figure legends.

References

1. Botuyan MV*, et al.* (2006) Structural basis for the methylation state-specific recognition of histone H4-K20 by 53BP1 and Crb2 in DNA repair. *Cell* 127(7):1361-1373.

2. Sanders SL*, et al.* (2004) Methylation of histone H4 lysine 20 controls recruitment of Crb2 to sites of DNA damage. *Cell* 119(5):603-614.

3. Sun Y*, et al.* (2009) Histone H3 methylation links DNA damage detection to activation of the tumour suppressor Tip60. *Nat Cell Biol* 11(11):1376-1382.

4. FARF Inc (2014) *Fanconi Anemia: Guidelines for Diagnosis and Management* (Fanconi Anemia Research Fund, Inc, Eugene, OR) Fourth Ed.

5. Mamrak NE, Shimamura A, & Howlett NG (2016) Recent discoveries in the molecular pathogenesis of the inherited bone marrow failure syndrome Fanconi anemia. *Blood Rev* 31(3):93-99

6. Knies K*, et al.* (2017) Biallelic mutations in the ubiquitin ligase *RFWD3* cause Fanconi anemia. *J Clin Invest in press*.

7. Kottemann MC & Smogorzewska A (2013) Fanconi anaemia and the repair of Watson and Crick DNA crosslinks. *Nature* 493(7432):356-363.

8. Walden H & Deans AJ (2014) The Fanconi anemia DNA repair pathway: structural and functional insights into a complex disorder. *Annu Rev Biophys* 43:257-278.

9. Alpi A*, et al.* (2007) UBE2T, the Fanconi anemia core complex, and FANCD2 are recruited independently to chromatin: a basis for the regulation of FANCD2 monoubiquitination. *Mol Cell Biol* 27(24):8421-8430.

10. Garcia-Higuera I*, et al.* (2001) Interaction of the Fanconi anemia proteins and BRCA1 in a common pathway. *Mol Cell* 7(2):249-262.

11. Sims AE*, et al.* (2007) FANCI is a second monoubiquitinated member of the Fanconi anemia pathway. *Nat Struct Mol Biol* 14(6):564-567.

12. Smogorzewska A*, et al.* (2007) Identification of the FANCI protein, a monoubiquitinated FANCD2 paralog required for DNA repair. *Cell* 129(2):289-301.

13. Marhold J, Brehm A, & Kramer K (2004) The Drosophila methyl-DNA binding protein MBD2/3 interacts with the NuRD complex via p55 and MI-2. *BMC Mol Biol* 5(1):20.

14. Martinez-Balbas MA, Tsukiyama T, Gdula D, & Wu C (1998) Drosophila NURF-55, a WD repeat protein involved in histone metabolism. *Proc Natl Acad Sci U S A* 95(1):132-137.

15. Nowak AJ*, et al.* (2011) Chromatin-modifying complex component Nurf55/p55 associates with histones H3 and H4 and polycomb repressive complex 2 subunit Su(z)12 through partially overlapping binding sites. *J Biol Chem* 286(26):23388-23396.

16. Song JJ, Garlick JD, & Kingston RE (2008) Structural basis of histone H4 recognition by p55. *Genes Dev* 22(10):1313-1318.

17. Trott O & Olson AJ (2010) AutoDock Vina: improving the speed and accuracy of docking with a new scoring function, efficient optimization, and multithreading. *J Comput Chem* 31(2):455-461.

18. Blus BJ, Wiggins K, & Khorasanizadeh S (2011) Epigenetic virtues of chromodomains. *Crit Rev Biochem Mol Biol* 46(6):507-526.

19. Du LL, Nakamura TM, & Russell P (2006) Histone modification-dependent and -independent pathways for recruitment of checkpoint protein Crb2 to double-strand breaks. *Genes Dev* 20(12):1583-1596.

20. Karachentsev D, Sarma K, Reinberg D, & Steward R (2005) PR-Set7-dependent methylation of histone H4 Lys 20 functions in repression of gene expression and is essential for mitosis. *Genes Dev* 19(4):431-435.

21. Nishioka K*, et al.* (2002) PR-Set7 is a nucleosome-specific methyltransferase that modifies lysine 20 of histone H4 and is associated with silent chromatin. *Mol Cell* 9(6):1201-1213.

22. Timmers C*, et al.* (2001) Positional cloning of a novel Fanconi anemia gene, *FANCD2*. *Mol Cell* 7:241-248.

23. Rogakou EP, Pilch DR, Orr AH, Ivanova VS, & Bonner WM (1998) DNA double-stranded breaks induce histone H2AX phosphorylation on serine 139. *J Biol Chem* 273(10):5858-5868.

24. Adamo A*, et al.* (2010) Preventing nonhomologous end joining suppresses DNA repair defects of Fanconi anemia. *Mol Cell* 39(1):25-35.

25. FitzGerald JE, Grenon M, & Lowndes NF (2009) 53BP1: function and mechanisms of focal recruitment. *Biochem Soc Trans* 37(Pt 4):897-904.

26. Yajima H, Lee KJ, & Chen BP (2006) ATR-dependent phosphorylation of DNA-dependent protein kinase catalytic subunit in response to UV-induced replication stress. *Mol Cell Biol* 26(20):7520-7528.

27. Zimmermann M & de Lange T (2014) 53BP1: pro choice in DNA repair. *Trends Cell Biol*. 24(2):108-117

28. Bakker ST, *et al.* (2009) Fancm-deficient mice reveal unique features of Fanconi anemia complementation group M. *Hum Mol Genet* 18(18):3484-3495.

29. Bunting SF, *et al.* (2012) BRCA1 functions independently of homologous recombination in DNA interstrand crosslink repair. *Mol Cell* 46(2):125-135.

30. Kim JM, *et al.* (2009) Inactivation of murine *Usp1* results in genomic instability and a Fanconi anemia phenotype. *Dev Cell* 16(2):314-320.

31. Vuono EA, *et al.* (2016) The PTEN phosphatase functions cooperatively with the Fanconi anemia proteins in DNA crosslink repair. *Sci Rep* 6:36439.

32. Jorgensen S, Schotta G, & Sorensen CS (2013) Histone H4 lysine 20 methylation: key player in epigenetic regulation of genomic integrity. *Nucleic Acids Res* 41(5):2797-2806.

33. Jorgensen S, *et al.* (2007) The histone methyltransferase SET8 is required for S-phase progression. *J Cell Biol* 179(7):1337-1345.

34. Oda H, *et al.* (2009) Monomethylation of histone H4-lysine 20 is involved in chromosome structure and stability and is essential for mouse development. *Mol Cell Biol* 29(8):2278-2295.

35. Sakaguchi A & Steward R (2007) Aberrant monomethylation of histone H4 lysine 20 activates the DNA damage checkpoint in Drosophila melanogaster. *J Cell Biol* 176(2):155-162.

36. Schotta G, *et al.* (2008) A chromatin-wide transition to H4K20 monomethylation impairs genome integrity and programmed DNA rearrangements in the mouse. *Genes Dev* 22(15):2048-2061.

37. Huyen Y*, et al.* (2004) Methylated lysine 79 of histone H3 targets 53BP1 to DNA double-strand breaks. *Nature* 432(7015):406-411.

38. Fradet-Turcotte A*, et al.* (2013) 53BP1 is a reader of the DNA-damage-induced H2A Lys 15 ubiquitin mark. *Nature* 499(7456):50-54.

39. Jacquet K*, et al.* (2016) The TIP60 complex regulates bivalent chromatin recognition by 53BP1 through direct H4K20me binding and H2AK15 acetylation. *Mol Cell* 62(3):409-421.

40. Tang J*, et al.* (2013) Acetylation limits 53BP1 association with damaged chromatin to promote homologous recombination. *Nat Struct Mol Biol* 20(3):317-325.

41. Rego MA, Kolling FW, Vuono EA, Mauro M, & Howlett NG (2012) Regulation of the Fanconi anemia pathway by a CUE ubiquitin-binding domain in the FANCD2 protein. *Blood* 120(10):2109-2117.

42. Bick G, Zhang F, Meetei AR, & Andreassen PR (2017) Coordination of the recruitment of the FANCD2 and PALB2 Fanconi anemia proteins by an ubiquitin signaling network. *Chromosoma* 126(3):417-430.

43. Long DT, Joukov V, Budzowska M, & Walter JC (2014) BRCA1 promotes unloading of the CMG helicase from a stalled DNA replication fork. *Mol Cell* 56(1):174-185.

44. Renaud E, Barascu A, & Rosselli F (2016) Impaired TIP60-mediated H4K16 acetylation accounts for the aberrant chromatin accumulation of 53BP1 and RAP80 in Fanconi anemia pathway-deficient cells. *Nucleic Acids Res* 44(2):648-656.

45. Nakanishi K*, et al.* (2011) Homology-directed Fanconi anemia pathway cross-link repair is dependent on DNA replication. *Nat Struct Mol Biol* 18(4):500-503.

46. Nakanishi K*, et al.* (2005) Human Fanconi anemia monoubiquitination pathway promotes homologous DNA repair. *Proc Natl Acad Sci U S A* 102(4):1110-1115.

47. Pace P*, et al.* (2010) Ku70 corrupts DNA repair in the absence of the Fanconi anemia pathway. *Science* 329(5988):219-223.

48. Knipscheer P*, et al.* (2009) The Fanconi anemia pathway promotes replication-dependent DNA interstrand cross-link repair. *Science* 326(5960):1698-1701.

49. Boisvert RA, Rego MA, Azzinaro PA, Mauro M, & Howlett NG (2013) Coordinate nuclear targeting of the FANCD2 and FANCI proteins via a FANCD2 nuclear localization signal. *PloS one* 8(11):e81387.

50. Howlett NG, Harney JA, Rego MA, Kolling FW, & Glover TW (2009) Functional interaction between the Fanconi Anemia D2 protein and proliferating cell nuclear antigen (PCNA) via a conserved putative PCNA interaction motif. *J Biol Chem* 284(42):28935-28942.

51. Liang CC*, et al.* (2016) The FANCD2-FANCI complex is recruited to DNA interstrand crosslinks before monoubiquitination of FANCD2. *Nature Commun* 7:12124.

APPENDIX-I

Conclusion

Upon DNA interstrand crosslink (ICL) formation, a core complex of FA proteins comes together to form an E2 and E3 ubiquitin ligase. This complex monoubiquitinates FANCD2, which is localized to sites of DNA damage. Monoubiquitinated FANCD2 then recruits downstream proteins to the break site, which are involved in removal of the ICL, and repair *via* homologous recombination (HR). The mechanism behind FANCD2 chromatin localization has remained poorly understood.

While histone posttranslational modification had been studied extensively in recent years, its role in damage repair has only just become evident. The H4K20me2 modification has been heavily implicated in DNA damage repair of double strand breaks, and is recognized by proteins involved in both error free repair *via* homologous recombination, and the error prone nonhomologous end joining pathway.

The focus of my dissertation has been elucidating how FANCD2 localizes to chromatin. Using *in silico* analysis, we determined that FANCD2 contained a histone binding and embedded methyl-binding domain. We confirmed that FANCD2 could bind to methylated H4K20 *in vitro* using purified FANCD2 in peptide and nucleosome pulldown assays. *In vivo*, we determined that FANCD2 associated with H4K20me2 upon ICL formation. Knockdown of the KMT5A enzyme, which monomethylates H4K20 (and is required for future dimethylation), is required for efficient FANCD2 chromatin localization and repair of ICLs. Using transformed patient cell lines which stably expressed wildtype or MBD mutant FANCD2, we determined the MBD is necessary for FANCD2 chromatin localization and tethering, and association with H4K20me2.

Additionally, mutation in the MBD resulted in increased, prolonged DNA damage, and increased presence of nonhomologous end joining markers, compared to wildtype expressing cells. Finally, MBD mutant cells failed to rescue sensitivity to MMC, shown by decreased cell survival and increased chromosomal aberrations compared to wildtype expressing cells. Our results indicate that upon ICL damage, FANCD2 is localized to sites of DNA damage *via* its MBD, where is binds specifically to H4K20me2 found at these sites.

APPENDIX-II

Supplemental information for Manuscript-II: "FANCD2 binding to H4K20me2 *via* a methyl-binding domain is essential for efficient DNA crosslink repair"

Supplementary information:

Materials and Methods

siRNA, Immunoblotting, and Antibodies

ON-TARGETplus SMARTpool siRNA against KMT5A (Dharmacon, L-031917-00-0005) was used for siRNA studies. HeLa cells were plated in six-well dishes at a density of 2 x 10^5 cells per well. The following day, cells were transfected with siRNA specific for KMT5A or control non-targeting siRNA using Lipofectamine 2000. Sixty-four h following transfection, cells were incubated in the absence or presence of 200 nM MMC or 1 μM APH for 16 h and harvested for analysis. For immunoblotting analysis, cell suspensions were washed in ice-cold PBS and lysed in SDS lysis buffer (2% v/v SDS, 50 mM Tris-HCl pH 7.4, 10 mM EDTA) with sonication. Proteins were resolved on NuPAGE 3-8% w/v Tris-Acetate or 4-12% w/v Bis-Tris gels (Invitrogen) and transferred to polyvinylidene difluoride (PVDF) membranes. The following mouse monoclonal antibodies were used: anti-GST (136700, Invitrogen), anti-γH2AX (05-636, Millipore), anti-α-Tubulin (MS-581-P1, NeoMarkers), anti-H4K20me1, anti-H4K20me2, anti-H4K20me3, anti-H3K27me3 and anti-V5 (R960-25, Invitrogen). Rabbit polyclonal antibodies used were: anti-53BP1 (sc-22760, Santa Cruz Biotechnology), anti-DNA-

PKcs pS2056 (ab18192, Abcam), anti-FANCD2 (NB100-182, Novus Biologicals), anti-FANCI (A300-212A and A300-254A, Bethyl Laboratories), anti-V5 (D3H8Q, Cell Signaling Technology), anti-H2A (07-146, Upstate), and anti-H3 (ab1791, Abcam).

Plasmids

Mutant cDNAs were generated using the Quikchange II site directed mutagenesis kit (Stratagene). The forward and reverse oligonucleotide sequences used are as follows: H1056A FP 5' CCAGGAGTGAAAGTTCAGGAGTACGCCATAATGTCTTCCTGC 3'; H1056A RP 5' GCAGGAAGACATTATGGCGTACTCCTGAACTTTCACTCCTGG 3'; W1075A FP 5' CATGGGCTTTTTGCTGCGAGTGGATTTTCTCAACCTG 3'; W1075A RP 5' CAGGTTGAGAAAATCCACTCGCAGCAAAAAGCCCATG 3'. The histone-binding domain (HBD) and methyl-binding domain (MBD) fragments were cloned into the pGEX-6P-1 plasmid using restriction enzyme cloning. The forward and reverse oligonucleotide sequences used are as follows: HBD FP 5' ATAGAATTCATGGATGAGCAGTGCACACAG 3'; HBD RP 5' TATCTCGAGTCACTCTGTGTGCTCCAGGTA 3'; MBD FP 5' ATAGAATTCATGTTTCATGGGCTTTTTG 3'; MBD RP 5' TATCTCGAGTCACAAAATAACCATCAAAAG 3'.

Protein Purification

GST-fusion proteins were expressed in BL21 Rosetta2 (DE3) pLysS cells following induction with isopropyl β-D-1-thiogalactopyranoside (IPTG) at 16°C. Cells were

pelleted, lysed in Buffer A (50 mM Tris-HCl pH 8.0, 150 mM NaCl, 1 mM EDTA, 1 mM PMSF, 1 mM DTT, 0.5% v/v NP-40, plus protease inhibitor cocktail tablets (Roche)) and flash frozen. The following day, cells were thawed on ice and lysed using a French press. Lysates were spun at 12,000 *g* for 30 min at 4°C and the supernatant filtered using a 0.45 μm filter. Glutathione agarose (Invitrogen) was applied to a column, and washed with deionized H_2O and Buffer A. Filtered supernatant was applied to the column. The column was washed in Buffer B (50 mM Tris-HCl pH 8.0, 750 mM NaCl, 0.5% v/v NP-40), and then Buffer A. Proteins were eluted at room temperature in Buffer C (50 mM Tris HCl pH 8.0, 150 mM NaCl, 0.5% v/v NP-40, and 20 mM reduced glutathione). Elution samples were resolved on NuPAGE 4-12% w/v Bis-Tris gels and stained with SimplyBlue SafeStain (Invitrogen). Protein-containing fractions were pooled and dialyzed against Buffer D (50 mM Tris-HCl pH 8.0, 150 mM NaCl, 0.05% v/v NP-40).

Chromatin Enrichment

Cells were plated at density of 3 x 10^6 cells in 15 cm^2 dishes. The following day, cells were treated with 200 nM mitomycin C (MMC) for 24 h. Cells were harvested and resuspended in ice-cold PBS. A portion of the pellet was set aside as the whole-cell lysate. The remaining pellet was lysed in ice-cold cytoskeletal buffer (CSK) (300 mM Sucrose, 100 mM NaCl, 3 mM $MgCl_2$, 0.5% v/v Triton-X-100, 1 mM EGTA, 10 mM PIPES, pH 6.8). The supernatant was collected as the soluble portion. The remaining pellet and whole-cell pellets were lysed in SDS lysis buffer with sonication.

Immunofluorescence Microscopy

Cells were plated at a density of 3 x 10^5 cells per well of culture slides (BDFalcon). The following day, cells were treated with 200 nM MMC for 24 h. Cells were pre-permeablized in permeabilization buffer (0.3% v/v Triton-X-100 in PBS pH 7.4) and fixed on ice in fixing buffer (4% w/v paraformaldehyde, 2% w/v sucrose, in PBS pH 7.4) for 15 min. Cells were permeabilized for 10 min, and blocked in antibody dilution buffer (ADB) (5% v/v Goat Serum, 0.1% v/v NP40 in PBS pH 7.4) for 30 min. Cells were stained for 1 h in primary antibody diluted in ADB, washed with PBS and permeabilization buffer, and stained with fluorescent secondary antibodies for 30 min in ADB. Cells were washed in PBS and permeablization buffer, and counterstained with 4′,6-Diamidino-2-phenylindole dihydrochloride (DAPI). Foci were analyzed using a Zeiss AxioImager.A1 upright epifluorescent microscope with AxioVision LE 4.6 image acquisition software. Proximity ligation assays (PLA) were performed similar to the immunofluorescence microscopy protocol up to the secondary antibody step. The remainder of the PLA protocol was carried out according to the manufacturers instructions (DUO92101,
Sigma Aldrich).

Mitomycin C Cell Survival Assay

Cells were plated at a density of 1.5 x 10^4 cells per well in 6-well dishes. The following day, cells were treated with varying concentrations of mitomycin C (MMC) for 7-10 days. Cells were washed in PBS and fixed in fixing buffer (10% v/v methanol, 10% v/v acetic acid). Cells were then stained with crystal violet (1% w/v crystal violet in methanol). The following day, the crystal violet was dissolved in dissolving solution

(0.02% v/v SDS in methanol) for 2 h. Solutions were transferred to 96 well dishes, and the OD_{570} was read using a 96-well Bio-Rad 680 microplate reader.

Chromosome Breakage Assay

For chromosome breakage assays, cells were grown in the absence or presence of 10 or 16 nM MMC for 24 h. Prior to harvesting, cells were treated with 0.1 μg/ml colcemid (Gibco/Invitrogen) for 2 h. Cell pellets were incubated in 0.075 M KCl at 37°C for 18 min, followed by fixation in Carnoy's fixative (3:1 methanol:glacial acetic acid) with multiple changes. Cells were dropped onto chilled slides and air-dried prior to staining with 3% v/v Giemsa solution (Sigma). Metaphases were analysed using a Zeiss AxioImager.A1 upright epifluorescent microscope with AxioVision LE 4.6 image acquisition software.

***In Vitro* Bulk Histone Binding Assays**

Glutathione agarose (Invitrogen) was blocked in NETN150 (20 mM Tris-HCl pH 7.5, 150 mM NaCl, 0.25% v/v NP-40, 1 mM EDTA) plus 1% w/v BSA, washed in NETN150 and added to GST-fusion proteins overnight at 4°C. Histones purified from calf thymus (Sigma) were pre-cleared with glutathione agarose at 4°C overnight. Precleared calf thymus histones were added to bead-bound GST-fusion proteins and incubated at 4°C for 1 h. Beads were washed 4x in NETN150 and bound proteins were eluted in 2x LDS/10% v/v β-mercaptoethanol with boiling. Bound proteins were resolved on 4-12% w/v Bis-Tris gels (Invitrogen) and stained with SimplyBlue SafeStain (Invitrogen), or H4K20me1, H4K20me2, or H4K20me3 antibodies.

Fig. S1. FANCD2 contains a putative histone-binding domain. (A) A BLASTp alignment of a short fragment of FANCD2 (aa 953-968) reveals homology with the histone H4 binding domain of Drosophila p55. A Clustal omega zoo multiple sequence alignment (MSA) of the FANCD2 histone-binding domain (HBD) illustrates strong evolutionary conservation. (B) AutoDock Vina molecular modeling was used to dock the H4 tail (taken from the p55-H4 crystal structure (PDB ID: 3C9C)) into the HBD of murine Fancd2 (PDB ID: 3S4W), indicating favorable H-bonding and electrostatic interactions between the H4 tail and the FANCD2 HBD. (C) Silver stain from an *in vitro* streptavidin sepharose pulldown assay with biotinylated histone peptides and GST-Empty and GST-D2-HBD. *, Non-specific bands present in all lanes, including bead only and no peptide controls. (D) Anti-GST immunoblot of (C). (E) Representative images of the FANCD2 methyl-lysine binding domain (MBD) aromatic cage with Kme2 manually docked. (F) Glutathione agarose pulldown of GST-tagged wild type MBD (GST-D2-MBD) and MBD-W1075A (GST-D2-MBD-W1075A) fragments incubated with purified histones from calf thymus (CTH). (G) Representative images of the proximity ligase assay (PLA) between FANCD2 and H4K20me1, me2, and me3. (H) Quantification of PLA results with 53BP1 and H4K20me1, me2, me3, and H3K27me3 in U2OS cells. Nuclei with >20 PLA spots were considered positive. At least 300 nuclei were scored per biological replicate. Experiments were performed three times with similar results. Error bars represent the standard errors of the means from three independent experiments. *, $P < 0.05$; **, $P < 0.01$; ***, $P < 0.001$.

A

```
H.sapiens FANCD2          EATEVVQLGPPELLFL
D.melanogaster p55        QSTEDAEDGPPELLFI

H.sapiens                 EATEVVQLGPPELLFLLEDLSQKLESMLTPPI
P.troglodytes             EATEVVQLGPPELLFLLEDLSQKLESMLTPPI
C.familiaris              EATEVVQLQPPELLFLLEDLSQKLENMLTPSV
G.gallus                  EASEVVQLGPAELCFLLDDMCWKLEHVLTPGS
M.musculus                EATEVVQLGPAELLFLLEDLSQKLENMLTAPF
R.norvegicus              EATEVVQLGPAELLFLLEDLSQKLENRLTPSF
X.laevis                  KATEVVQLGPAELVFLLEDLFRKTENILTS-A
D.rerio                   KLREEVQLGPAELLFLLEDMWRKLDFSLTSAP
```

B

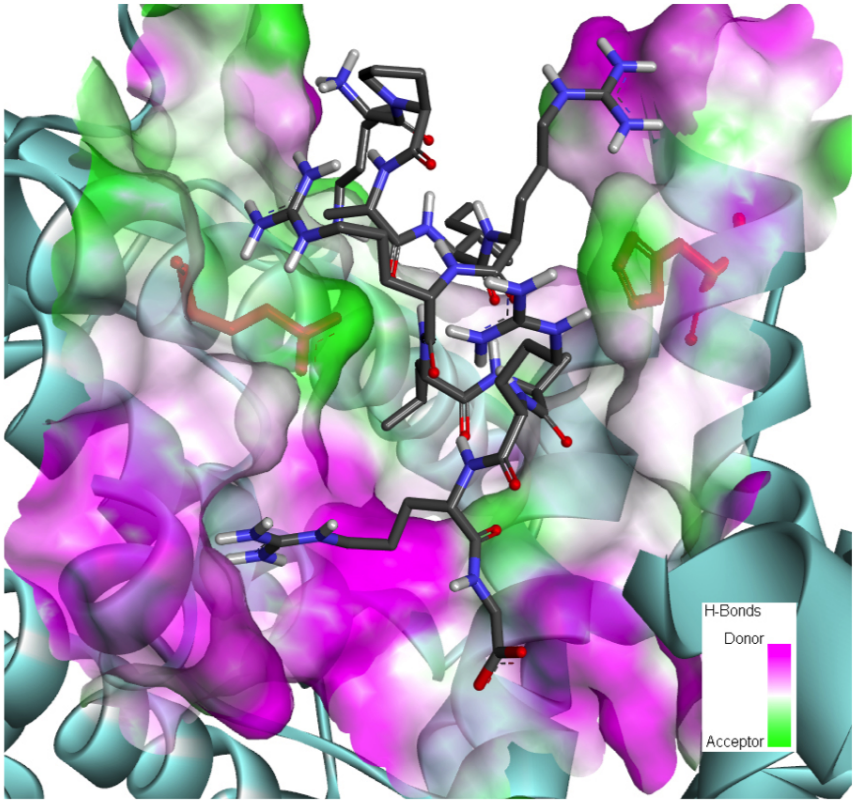

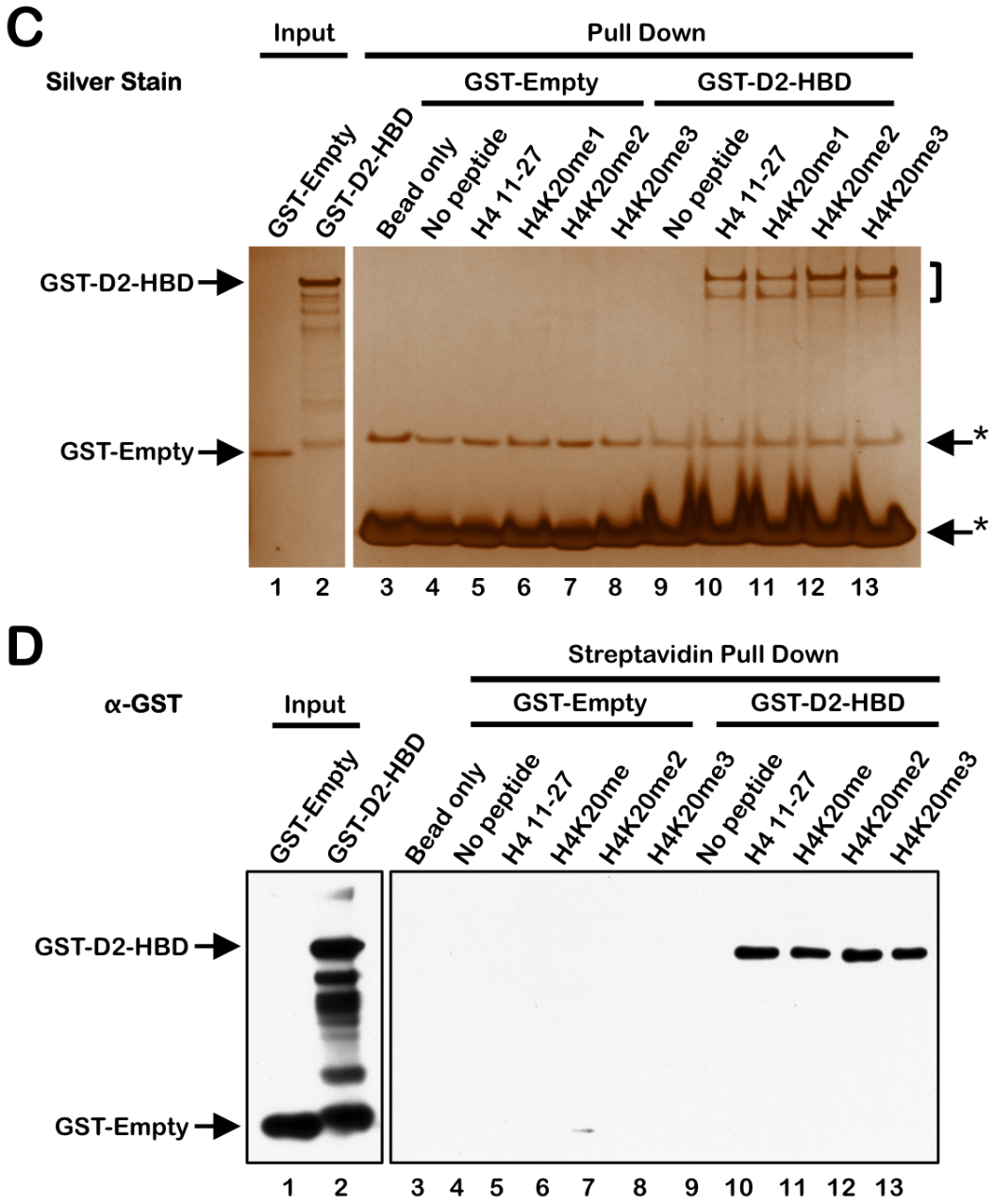
C
Silver Stain
Input
Pull Down
GST-Empty
GST-D2-HBD
GST-Empty
GST-D2-HBD
Bead only
No peptide
H4 11-27
H4K20me1
H4K20me2
H4K20me3
No peptide
H4 11-27
H4K20me1
H4K20me2
H4K20me3
GST-D2-HBD
GST-Empty
*
*
1 2 3 4 5 6 7 8 9 10 11 12 13
D
α-GST
Input
Streptavidin Pull Down
GST-Empty
GST-D2-HBD
GST-Empty
GST-D2-HBD
Bead only
No peptide
H4 11-27
H4K20me
H4K20me2
H4K20me3
No peptide
H4 11-27
H4K20me
H4K20me2
H4K20me3
GST-D2-HBD
GST-Empty
1 2 3 4 5 6 7 8 9 10 11 12 13

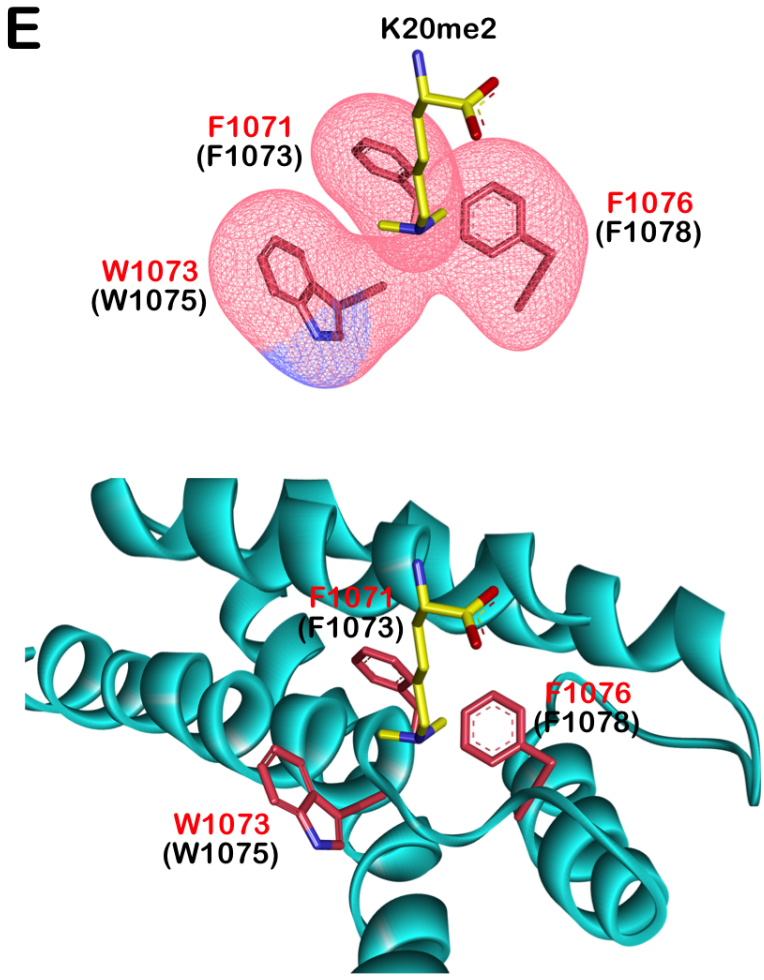
E
K20me2
F1071
(F1073)
F1076
(F1078)
W1073
(W1075)
F1071
(F1073)
F1076
(F1078)
W1073
(W1075)

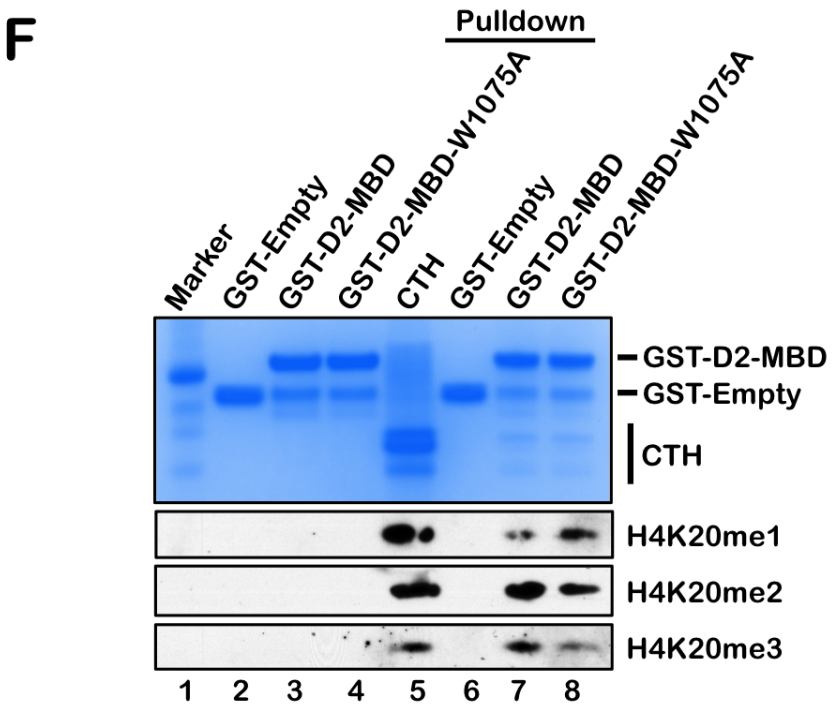
F
Pulldown
Marker
GST-Empty
GST-D2-MBD
GST-D2-MBD-W1075A
CTH
GST-Empty
GST-D2-MBD
GST-D2-MBD-W1075A
GST-D2-MBD
GST-Empty
CTH
H4K20me1
H4K20me2
H4K20me3
1 2 3 4 5 6 7 8

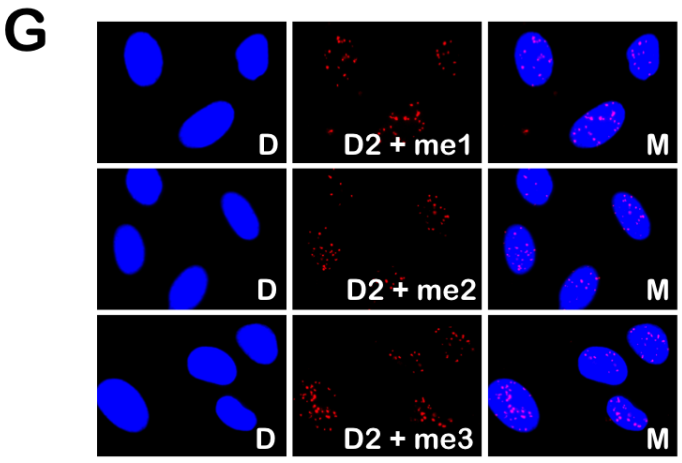
G
D
D2 + me1
M
D
D2 + me2
M
D
D2 + me3
M

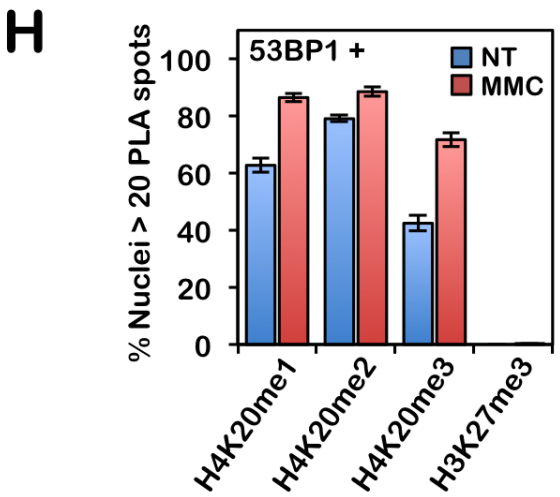
H
% Nuclei > 20 PLA spots
100
80
60
40
20
0
53BP1 +
NT
MMC
H4K20me1
H4K20me2
H4K20me3
H3K27me3

Fig. S2. The histone methyltransferase KMT5A is necessary for efficient activation of the FA pathway. (A) MCF10A cells were incubated with control non-targeting siRNA (siControl) or siRNA targeting KMT5A (siKMT5A) for 72 h. Cells were then treated with 200 nM mitomycin C (MMC) or 1 μM aphidicolin (APH) for 16 h and whole-cell lysates analyzed by immunoblotting. L:S ratio, ratio of monoubiquitinated to nonubiquitinated FANCD2 or FANCI (B) Representative images of FANCD2 foci in MMC-treated MCF10A cells. Cells were treated as described in (A). D, DAPI; D2; FANCD2; M, merge. (C) Quantification of FANCD2 foci formation for (B). Nuclei with > 10 FANCD2 foci were considered positive. At least 300 nuclei were scored per biological replicate. Experiments were performed twice with similar results. Error bars represent the standard errors of the means from three independent experiments. *, $P < 0.05$; **, $P < 0.01$; ***, $P < 0.001$.

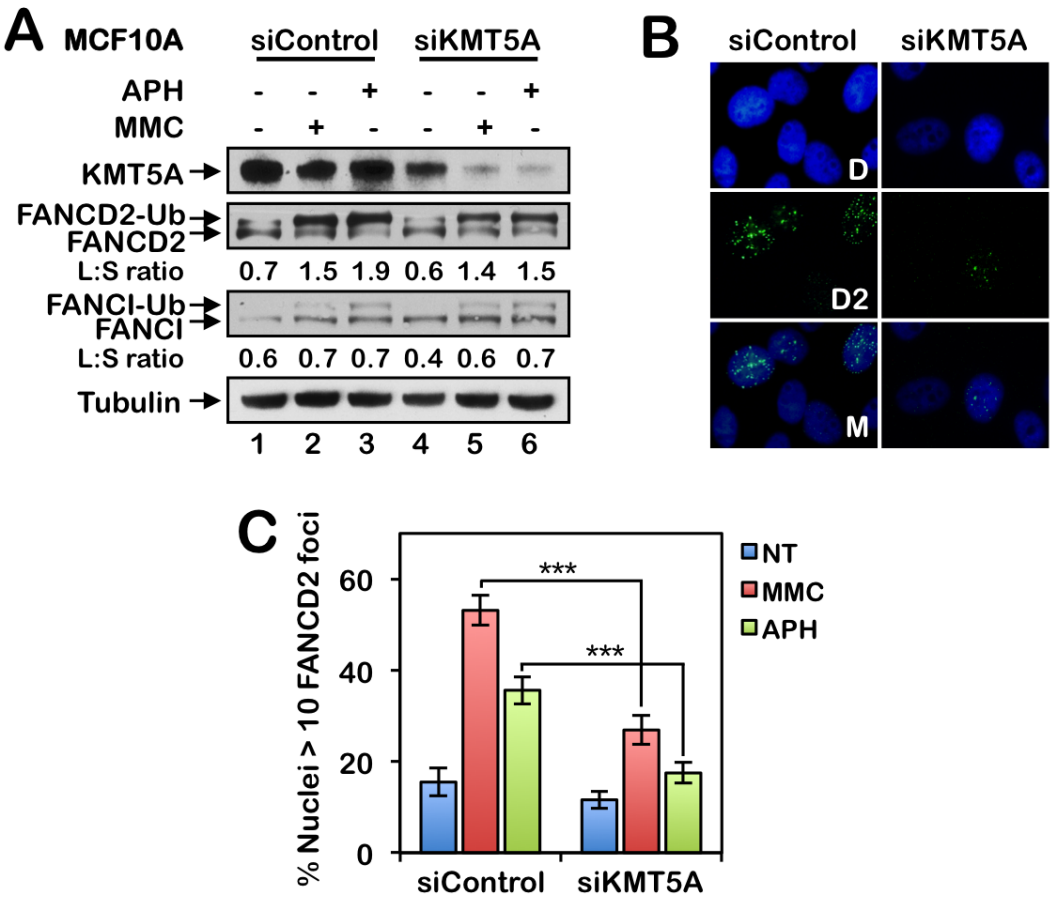
A
MCF10A
siControl
siKMT5A
APH
MMC
KMT5A
FANCD2-Ub
FANCD2
L:S ratio
0.7 1.5 1.9 0.6 1.4 1.5
FANCI-Ub
FANCI
L:S ratio
0.6 0.7 0.7 0.4 0.6 0.7
Tubulin
1 2 3 4 5 6
B
siControl
siKMT5A
D
D2
M
C
% Nuclei > 10 FANCD2 foci
60
40
20
0
***
***
NT
MMC
APH
siControl
siKMT5A

Fig. S3. FANCD2 MBD mutants are proficient for monoubiquitination but exhibit decreased affinity for chromatin. (A) FA-D2 cells stably expressing wild type FANCD2, FANCD2-H1056A, and FANCD2-W1075A were incubated in the absence (-) or presence (+) of 200 nM mitomycin C (MMC) for 24 h. A chromatin enrichment fractionation was performed and soluble and chromatin-enriched fractions were analyzed by immunoblotting. (B) The same cells were treated as for (A) and nuclear fractions were extracted in buffers containing varying NaCl concentrations (see Fig. 3B). Whole-cell lysates from this experiment are shown. (C) Quantification of the protein band intensities from Fig. 3B calculated from three independent experiments. The Y-axis depicts the ratios of band intensities compared to the band from FA-D2 cells expressing wild type FANCD2 at the equivalent NaCl concentration.

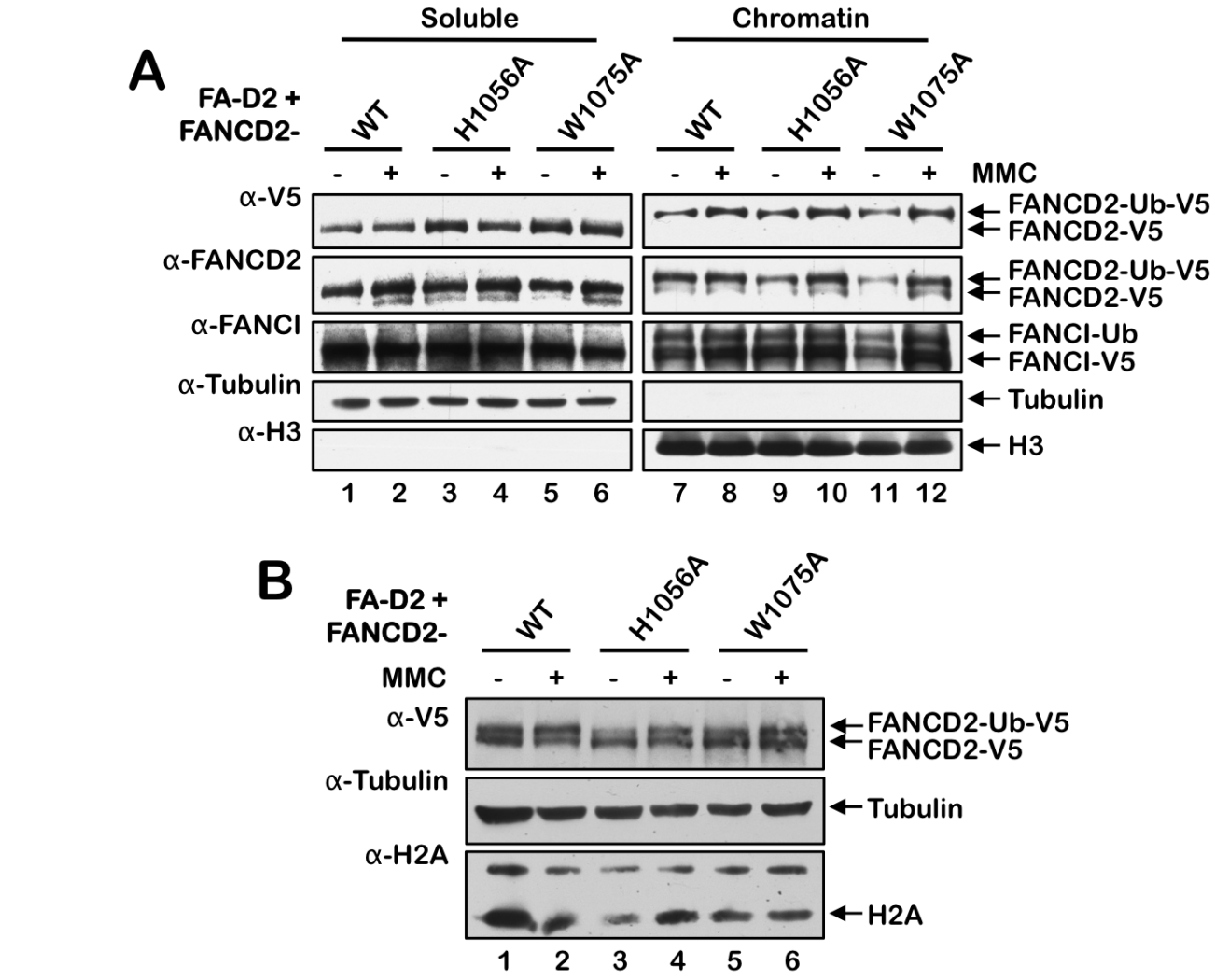
A
Soluble
Chromatin
FA-D2 +
FANCD2-
WT
H1056A
W1075A
WT
H1056A
W1075A
- + - + - + - + - + - +
MMC
α-V5
α-FANCD2
α-FANCI
α-Tubulin
α-H3
FANCD2-Ub-V5
FANCD2-V5
FANCD2-Ub-V5
FANCD2-V5
FANCI-Ub
FANCI-V5
Tubulin
H3
1 2 3 4 5 6 7 8 9 10 11 12
B
FA-D2 +
FANCD2-
WT
H1056A
W1075A
MMC
- + - + - +
α-V5
α-Tubulin
α-H2A
FANCD2-Ub-V5
FANCD2-V5
Tubulin
H2A
1 2 3 4 5 6
C
Fold change relative to WT signal
NT 150 mM NaCl
MMC 150 mM NaCl
NT 250 mM NaCl
MMC 250 mM NaCl
NT 500 mM NaCl
MMC 500 mM NaCl
0
0.5
1
1.5
2
2.5
3
WT
H1056A
W1075A

Fig. S4. Mutation of the FANCD2 MBD leads to increased association between 53BP1 and H4K20me2 and me3. Quantification of proximity ligation assay (PLA) results with 53BP1 and H4K20me1, me2, me3, and H3K27me3 in FA-D2 cells stably expressing wild type FANCD2 or FANCD2-W1075A. Nuclei with >20 PLA spots were considered positive. At least 300 nuclei were scored per biological replicate. Experiments were performed three times with similar results. Error bars represent the standard errors of the means from three independent experiments. *, $P < 0.05$; **, $P < 0.01$; ***, $P < 0.001$.

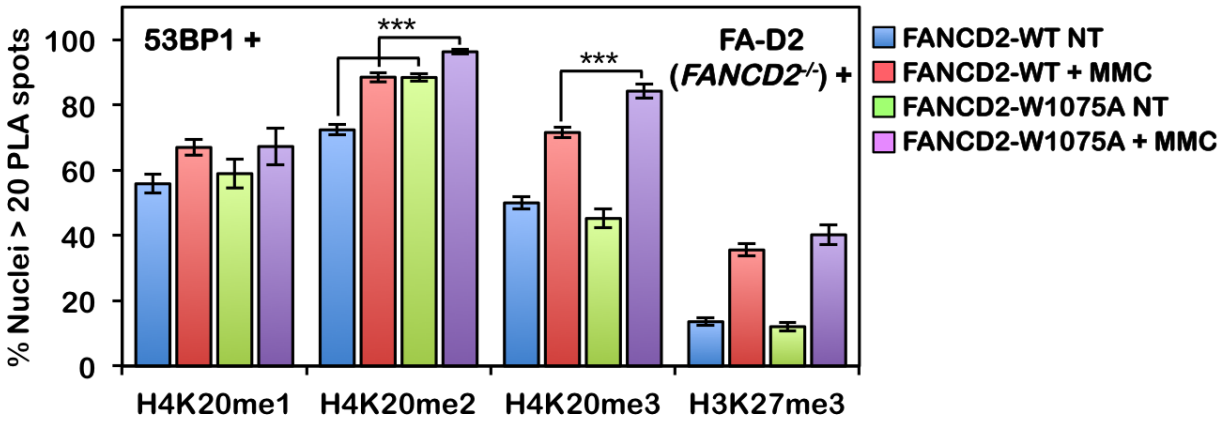
53BP1 +
FA-D2
(FANCD2-/-) +
***
***
% Nuclei > 20 PLA spots
100
80
60
40
20
0
H4K20me1
H4K20me2
H4K20me3
H3K27me3
FANCD2-WT NT
FANCD2-WT + MMC
FANCD2-W1075A NT
FANCD2-W1075A + MMC

Fig. S5. The FANCD2 HBD/MBD is required for efficient conservative ICL repair. (A) FA-D2 cells stably expressing LacZ, wild type FANCD2, FANCD2-K561R, FANCD2-H1056A, and FANCD2-W1075A were incubated in the absence (NT) or presence (+MMC) of 16 nM mitomycin C (MMC) for 24 h and metaphase chromosomes analyzed for structural aberrations, including gaps, breaks and radial formations. Representative metaphases are shown. Blue arrows depict gaps and breaks while red arrows depict more complex radial formations. (B) The same cells were incubated in the absence (NT) or presence (MMC) of 200 nM MMC for 24 h and allowed to recover for an additional 24 h. Cells were fixed and stained with anti-DNA-PKcs pS2056 antibodies and the numbers of nuclei with >5 foci were scored. At least 300 nuclei were scored per biological replicate. *, $P < 0.05$; **, $P < 0.01$; ***, $P < 0.001$. (C) A growth curve was carried out with the same cells with cell counts taken every 24 h over a 96 h period. Experiments were performed three times with similar results. Error bars represent the standard errors of the means from three independent experiments.

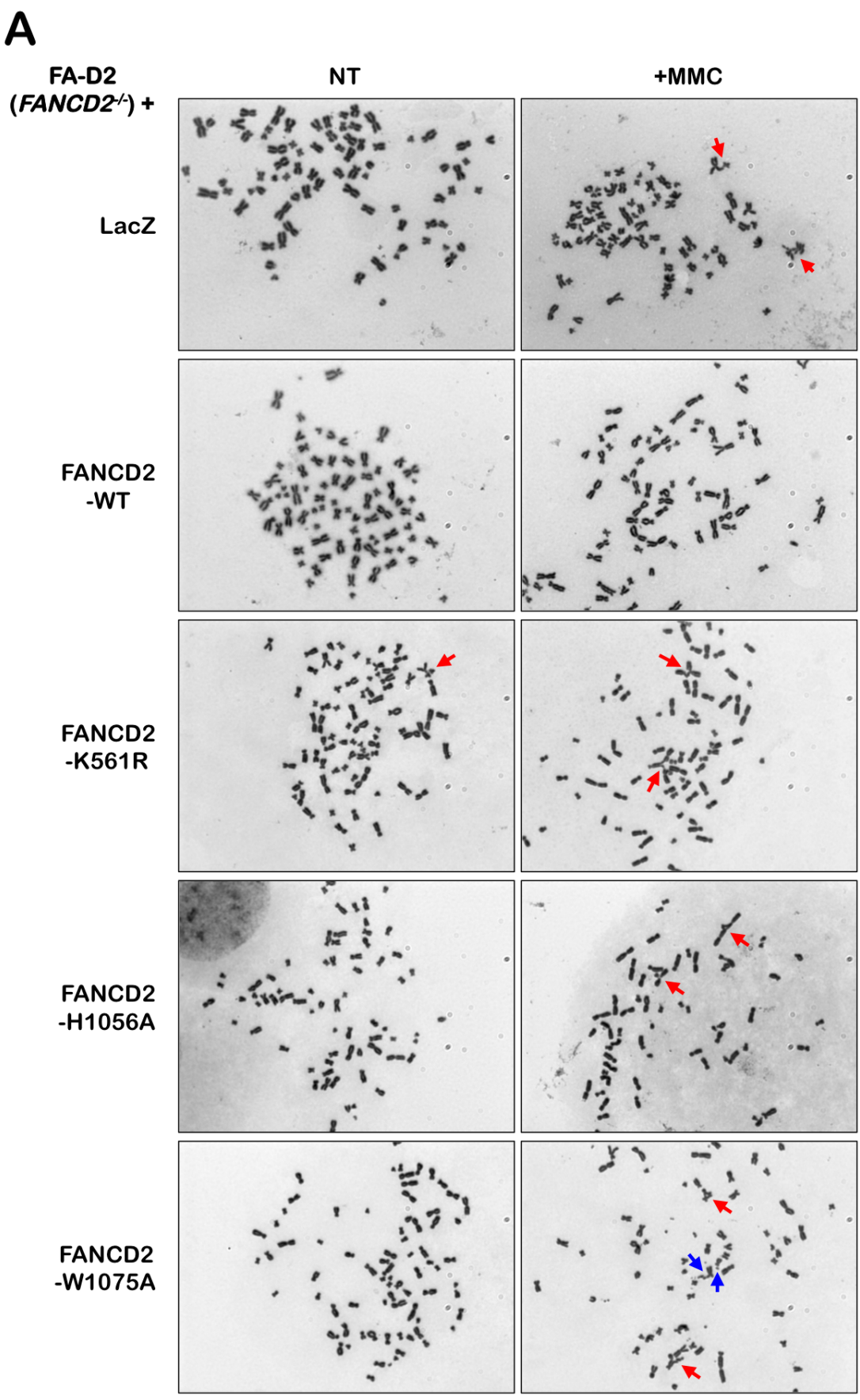
A
FA-D2
(FANCD2-/-) +
NT
+MMC
LacZ
FANCD2
-WT
FANCD2
-K561R
FANCD2
-H1056A
FANCD2
-W1075A

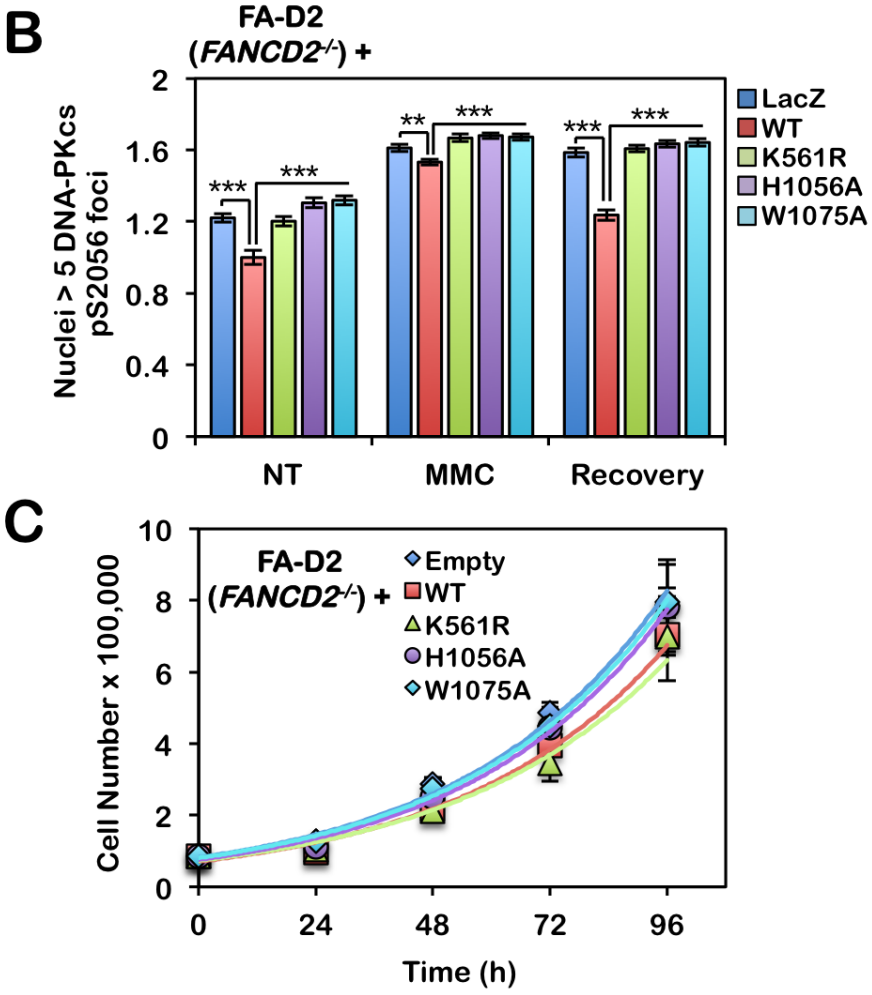
B
FA-D2
(FANCD2-/-) +
Nuclei > 5 DNA-PKcs pS2056 foci
2
1.6
1.2
0.8
0.4
0
***
***
**
***
***
***
LacZ
WT
K561R
H1056A
W1075A
NT
MMC
Recovery
C
FA-D2
(FANCD2-/-) +
Empty
WT
K561R
H1056A
W1075A
Cell Number x 100,000
10
8
6
4
2
0
0
24
48
72
96
Time (h)

APPENDIX-III

Published in Cell Cycle, 2016

A DUB-less step? Tighten up D-loop

Karissa L. Paquin* , David A. Vierra* , and Niall G. Howlett1

Department of Cell and Molecular Biology, University of Rhode Island, Kingston, RI, USA

Department of Cell and Molecular Biology, University of Rhode Island, Kingston, Rhode Island, U.S.A

*These authors equally contributed to this work

[1]Corresponding author: Niall G. Howlett Ph.D., 379 Center for Biotechnology and Life Sciences, 120 Flagg Road, Kingston, RI, USA, Tel.: +1 401 874 4306; Fax: +1 401 874 2065; *Email address*: **nhowlett@uri.edu**

Keywords: DNA repair; Fanconi anemia; homologous recombination; ubiquitin

A DUB-less step? Tighten up D-loop

Karissa L. Paquin* , David A. Vierra* , and Niall G. Howlett1

Department of Cell and Molecular Biology, University of Rhode Island, Kingston, RI, USA

Department of Cell and Molecular Biology, University of Rhode Island, Kingston, Rhode Island, U.S.A

*These authors equally contributed to this work

[1]Corresponding author: Niall G. Howlett Ph.D., 379 Center for Biotechnology and Life Sciences, 120 Flagg Road, Kingston, RI, USA, Tel.: +1 401 874 4306; Fax: +1 401 874 2065; *Email address*: **nhowlett@uri.edu**

Keywords: DNA repair; Fanconi anemia; homologous recombination; ubiquitin

DNA double-strand breaks (DSBs) can arise through exposure to exogenous DNA damaging agents such as ionizing radiation, as well as through endogenous means; for example, via DNA replication fork collapse. Irrespective of the source, the physical severing of the sugar-phosphate backbone represents an acute threat to organismal viability and genome stability. Hanahan and Weinberg describe genome instability and mutation as an enabling characteristic of cancer.1 Indeed, chromosome structural rearrangements, which are pervasive in cancer, invariably arise from DSB repair gone awry. To deal with this threat, all cells have evolved 2 principal means to repair DSBs: homologous recombination (HR) and nonhomologous DNA end joining (NHEJ). HR is predominantly a conservative and error-free process, employing a homologous template, usually the sister chromatid, to repair the break. RAD51, the eukaryotic ortholog of bacterial RecA, is the major HR protein. Conversely, NHEJ is typically error-prone, and rejoins the break without regard for the state of the ends, often resulting in loss of nucleotides or the re-joining of noncontiguous ends. Exemplifying the importance of HR, many key tumor suppressor genes encode central HR players, e.g. BRCA1 and BRCA2. Furthermore, several genetic diseases characterized by increased cancer risk are caused by mutations in HR genes, one example of which is Fanconi anemia (FA).

FA is clinically characterized by congenital defects, bone marrow failure, and increased cancer risk.2 FA is caused by mutation of any one of 20 known genes, which encode proteins that function cooperatively in the FA-BRCA pathway to promote HR.3 The molecular links between FA and HR are an area of active investigation. Evidence presented in this volume of Cell Cycle points to a novel noncanonical connection between enzymes involved in the major regulatory step of the FA-BRCA pathway and a

key HR effector.4 This regulatory step is the site-specific monoubiquitination of the FANCD2 and FANCI proteins. The E2 ubiquitin-conjugating enzyme FANCT/UBE2T and the E3 ubiquitin ligase FANCL catalyze the forward step of this reaction. The reverse step - deubiquitination - is catalyzed by the USP1 deubiquitinating enzyme (DUB) and its heterodimeric binding partner UAF1.5,6

In a large-scale global proteomic screen of DUB-interacting networks, Sowa et al. previously determined that the USP1- UAF1 heterodimer interacts with the RAD51AP1 protein.7 RAD51AP1 is a vertebrate specific accessory factor for RAD51 that promotes the assembly of the synaptic complex and D (displacement)-loop, key HR intermediate structures (Fig. 1). However, the functional significance of this interaction was not examined. In the accompanying Cell Cycle manuscript, Cukras et al. have tackled this important question.4 The authors verified this interaction and, by depleting UAF1 using siRNA, established that the interaction between USP1 and RAD51AP1 is UAF1-dependent. The authors also established that the UAF1 WD40 repeats as well as its SUMO-like domains (SLDs) are necessary for RAD51AP1 binding. Previous studies had demonstrated that USP1 regulates the stability of the ID (inhibitor of DNA binding) proteins. Similarly, Cukras et al. show that depletion of USP1 or UAF1 leads to destabilization of RAD51AP1.

Cukras et al. next sought to map the region of RAD51AP1 that binds to UAF1. Serial truncations and mutagenesis analysis established that residues D133-L137 are required for efficient RAD51AP1-UAF1 binding. Accordingly, deletion of this UAF1 binding region (DDYLDL) resulted in decreased RAD51AP1 stability, supporting the theory that USP1-UAF1-RAD51AP1 form a stable protein complex. Interestingly,

Figure 1. Speculative schematic of the role of the USP1-UAF1-RAD51AP1 complex in HR. UAF1 binds to USP1through its WD40 domain, and RAD51AP1 through its SLD1/ 2 domains. In the absence of either UAF1 or USP1, RAD51AP1 is degraded by the proteasome. Following RAD51 nucleofilament formation, RAD51AP1 is required for synaptic complex and D-loop formation. This is promoted by the presence of UAF1, however the role of USP1 in this process remains unclear. On the right side of this figure, USP1 is depicted in gray font to signify its uncertain role in this process.

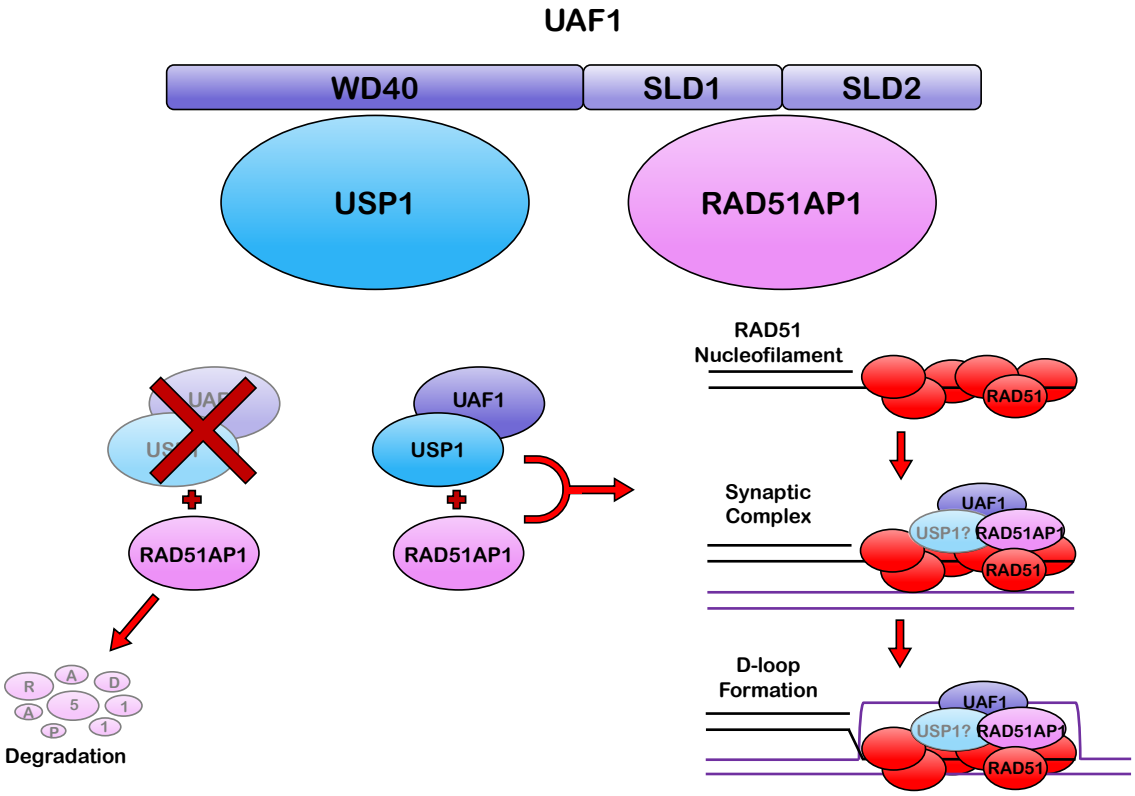
UAF1
WD40
SLD1
SLD2
USP1
RAD51AP1
RAD51AP1
UAF1
USP1
RAD51AP1
Degradation
RAD51
Nucleofilament
RAD51
Synaptic
Complex
UAF1
USP1?
RAD51AP1
RAD51
D-loop
Formation
UAF1
USP1?
RAD51AP1
RAD51

mutation of RAD51AP1 K139, previously shown to be a site of ubiquitination, did not affect interaction with UAF1. To explore the functional significance of the RAD51AP1-UAF1 interaction, Cukras et al. expressed wild type or RAD51AP1-DDYLDL in U2OS cells depleted of endogenous RAD51AP1. In contrast to wild type RAD51AP1, the DDYLDL mutant failed to correct cellular ICL sensitivity. Furthermore, RAD51AP1-DDYLDL expressing cells exhibited persistent DNA damage-inducible RAD51 nuclear foci, suggesting that the USP1-UAF1-RAD51AP1 complex may promote the efficient and timely resolution of a key HR intermediate structure.

A recent complementary study in Cell Reports by Liang et al. provides further insight into the functional significance of the RAD51AP1-UAF1 interaction.8 Similar to Cukras et al., Liang et al. establish that the UAF1 SLDs mediate interaction with RAD51AP1. While mutation of these SLDs compromises interaction with RAD51AP1, these mutants are proficient for interaction with USP1 and stimulation of its DUB activity toward FANCD2. Importantly, Liang et al. also establish that UAF1 alone stimulates the ability of RAD51AP1 to promote synaptic complex and D-loop formation in vitro, and this stimulation depends on the formation of the RAD51AP1-UAF1 complex. These assays indicate that UAF1-stimulated RAD51AP1 activity is largely USP1-independent. While Cukras et al. clearly show that USP1 forms a complex with UAF1 and RAD51AP1, a role for enzymatic deubiquitination has not been established. Taken together, these studies reveal a novel and critical function for UAF1 in promoting HR that appears to be independent of USP1 deubiquitinating activity. However, it remains to be determined how RAD51AP1 is removed from RAD51 nucleoprotein filaments enabling the dissolution of HR intermediates - ubiquitination remains a plausible

mechanism. In conclusion, these studies uncover important mechanistic insight into the molecular biology of HR and FA and suggest the existence of more FA genes linked to the regulation of RAD51 function.

Disclosure of potential conflicts of interest

No potential conflicts of interest were disclosed.

Funding

This work was supported by National Institutes of Health/National Heart, Lung and Blood Institute grant R01HL101977 to NGH, and Rhode Island IDeA Network of Biomedical Research Excellence (RI-INBRE) grant P20GM103430 from the National Institute of General Medical Sciences.

References

[1] Hanahan D, Weinberg RA. Hallmarks of cancer: the next generation. Cell 2011; 144:646-74; PMID:21376230; http://dx.doi.org/10.1016/j. cell.2011.02.013

[2] Fund FAR. Fanconi anemia: guidelines for diagnosis and management. 4th ed. Eugene, OR: Fanconi Anemia Research Fund; 2014; 1-429.

[3] Walden H, Deans AJ. The Fanconi anemia DNA repair pathway: structural and functional insights into a complex disorder. Annu Rev Biophys 2014; 43:257-78; PMID:24773018; http://dx.doi.org/10.1146/ annurev-biophys-051013-022737

[4] Cukras S, Lee E, Palumbo P, Benavidez P, Moldovan GL, Kee Y. The USP1-UAF1 complex interacts with RAD51AP1 to promote homologous recombination repair. Cell Cycle 2016; 15(19):2636-2646; PMID: 27463890; http://dx.doi.org/10.1080/15384101.2016.1209613

[5] Cohn MA, Kowal P, Yang K, Haas W, Huang TT, Gygi SP, D'Andrea AD. A UAF1-containing multisubunit protein complex regulates the Fanconi anemia pathway. Mol Cell 2007; 28:786-97; PMID:18082604; http://dx.doi.org/10.1016/j.molcel.2007.09.031

[6] Nijman SM, Huang TT, Dirac AM, Brummelkamp TR, Kerkhoven RM, D'Andrea AD, Bernards R. The deubiquitinating enzyme USP1 regulates the Fanconi anemia pathway. Mol Cell 2005; 17:331-9; PMID:15694335; http://dx.doi.org/10.1016/j.molcel. 2005.01.008

[7] Sowa ME, Bennett EJ, Gygi SP, Harper JW. Defining the human deubiquitinating enzyme interaction landscape. Cell 2009; 138:389-403; PMID:19615732; http://dx.doi.org/10.1016/j.cell.2009. 04.042

[8] Liang F, Longerich S, Miller AS, Tang C, Buzovetsky O, Xiong Y, Maranon DG, Wiese C, Kupfer GM, Sung P. Promotion of RAD51- mediated homologous DNA pairing by the RAD51AP1-UAF1 complex. Cell Rep 2016; 15:2118-26; PMID:27239033; http://dx.doi. org/10.1016/j.celrep.2016.05.007